EARTH OBSERVATION FOR SDG TARGETS AND INDICATORS, LOT-1

SDG 15.2.1 EO PATHFINDER: EO FOR SUSTAINABLE FOREST MANAGEMENT

D3.2 Algorithm Theoretical Baseline Documents

ESA Contract No: 4000139583/22/I-DT
IABG Ref.: TA-B- 004219
Date: 2024/12/18
Issue: v1.0

15

esa

E04SDG-Forest

SUSTAINABLE FOREST MANAGEMENT

IABG rss Sertit ICUBE VTT

< PAGE INTENTIONALLY LEFT BLANK >

Document status

Version	Date	Organisation(s) Author(s)
1.0	2024/03/22	Dzhaner Emin (IABG) Andrés Andrade (IABG) Jose Cortes (IABG) Dr. Maximilian Schwarz (RSS) Henri Giraud (SERTIT)

Document change directory

Version	Date	Description	Section/ page

Table of Contents

List of Figures

List of Tables

Acronyms and Abbreviations

Abbr.	Description
EA	Early Adopter
EO	Earth Observation
ESA	European Space Agency
SDG	Sustainable Development Goals
TEP	Forestry Thematic Exploitation Platform
WB	World Bank
SWIR	short wavelength infrared
NIR	Near infrared
VI	Vegetation Index / Indices
NDVI	Normalized Difference Vegetation Index
CVA	Change Vector Analysis
BFAST	Breaks For Additive Seasonal and Trend

Abbr.	Description

Applicable Documents

Ref.	Title	Version	Date
[AD01]	Ref.: EOP-SD-SOW-0158 Statement of Work ESA Express Procurement - [EXPRO+], Earth Observation for SDG Targets and Indicators Lot-1	1.0	2021/10/14
[AD02]	Sinha, P., Kumar, L., & Reid, N. (2016). Rank-based methods for selection of landscape metrics for land cover pattern change detection. *Remote Sensing, 8*(2), 107. https://doi.org/10.3390/rs8020107		2016
[AD03]	De Clercq, E. M., Vandemoortele, F., & De Wulf, R. R. (2006). A method for the selection of relevant pattern indices for monitoring of spatial forest cover pattern at a regional scale. *International Journal of Applied Earth Observation and Geoinformation, 8*(2), 113-125. https://doi.org/10.1016/j.jag.2005.07.002		2006
[AD04]	Diaz-Varela, E. R., Marey-Pérez, M. F., Rigueiro-Rodriguez, A., & Álvarez-Álvarez, P. (2009). Landscape metrics for characterization of forest landscapes in a sustainable management framework: potential application and prevention of misuse. *Annals of forest science, 66*(3), 1-10. https://doi.org/10.1051/forest/2009004		2009
[AD05]	Uwiringiyimana, H., & Choi, J. (2022). Remote Sensing and Landscape Metrics-Based Forest Physical Degradation: Two-Decades Assessment in Gishwati-Mukura Biological Corridor in Rwanda, East-Central Africa. *Journal of Geoscience and Environment Protection, 10*(4), 64-81. https://doi.org/10.4236/gep.2022.104005		2022
[AD06]	Shao, S., Yu, M., Huang, Y., Wang, Y., Tian, J., & Ren, C. (2022). Towards a Core Set of Landscape Metrics of Urban Land Use in Wuhan, China. *ISPRS International Journal of Geo-Information, 11*(5), 281. https://doi.org/10.3390/ijgi11050281		2022
[AD07]	Uuemaa, E., Antrop, M., Roosaare, J., Marja, R., & Mander, Ü. (2009). Landscape metrics and indices: an overview of their use in landscape research. *Living reviews in landscape research, 3*(1), 1-28. http://dx.doi.org/10.12942/lrlr-2009-1		2009
[AD08]	Dormann, C. F., Elith, J., Bacher, S., Buchmann, C., Carl, G., Carré, G., ... & Lautenbach, S. (2013). Collinearity: a review of methods to deal with it and a simulation study evaluating their performance. *Ecography, 36*(1), 27-46. https://doi.org/10.1111/j.1600-0587.2012.07348.x		2013
[AD09]	Hargis, C. D., Bissonette, J. A., & David, J. L. (1998). The behavior of landscape metrics commonly used in the study of habitat fragmentation. *Landscape ecology, 13*, 167-186. https://doi.org/10.1023/A:1007965018633		1998
[AD10]	Ishan (2023). Choosing the Right Correlation: Pearson vs. Spearman vs. Kendall's Tau. Medium. https://ishanjainoffical.medium.com/choosing-the-right-correlation-pearson-vs-spearman-vs-kendalls-tau-02dc7d7dd01d		2023

Ref.	Title	Version	Date
[AD11]	Forman, R.T.T.; Godron, M. (1986). *Landscape ecology*. New York: John Wiley & Sons. 619 p.		1986
[AD12]	Turner, M. G. (1989). Landscape ecology: the effect of pattern on process. *Annual review of ecology and systematics, 20*(1), 171-197. https://doi.org/10.1146/annurev.es.20.110189.001131		1989
[AD13]	Urban, D.L.; O'Neill, R.V.; Shugart, Jr., H.H. (1987). Landscape ecology: a hierarchical perspective can help scientist understand spatial patterns. *BioScience. 37*, 119-127.		1987
[AD14]	Saunders, D. A., Hobbs, R. J., & Margules, C. R. (1991). Biological consequences of ecosystem fragmentation: a review. *Conservation biology, 5*(1), 18-32. DOI:10.1111/j.1523-1739.1991.tb00384.x		1991
[AD15]	Harris, L. D. (1984). *The fragmented forest: island biogeography theory and the preservation of biotic diversity*. University of Chicago press.		1984
[AD16]	Dunning, J. B., Danielson, B. J., & Pulliam, H. R. (1992). Ecological processes that affect populations in complex landscapes. *Oikos*, 169-175. https://doi.org/10.2307/3544901		1992
[AD17]	MacArthur, R. H., & Wilson, E. O. (2001). *The theory of island biogeography* (Vol. 1). Princeton University Press.		2001
[AD18]	Risser, P. G., Karr, J. R., & Forman, R. T. (1984). Landscape ecology: directions and approaches: a workshop held at Allerton Park, Piatt County, Illinois, April 1983. *Illinois Natural History Survey Special Publication no. 02*.		1984
[AD19]	Wiens, J. A. (1976). Population responses to patchy environments. *Annual review of ecology and systematics, 7*(1), 81-120.		1976
[AD20]	Kotliar, N. B., & Wiens, J. A. (1990). Multiple scales of patchiness and patch structure: a hierarchical framework for the study of heterogeneity. *Oikos*, 253-260.		1990
[AD21]	Kolasa, J., Rollo, C.D. (1991). Introduction: The Heterogeneity of Heterogeneity: A Glossary. In: Kolasa, J., Pickett, S.T.A. (eds) *Ecological Heterogeneity*. Ecological Studies, vol 86. Springer, New York, NY. https://doi.org/10.1007/978-1-4612-3062-5_1		1991
[AD22]	Li, X., He, H. S., Bu, R., Wen, Q., Chang, Y., Hu, Y., & Li, Y. (2005). The adequacy of different landscape metrics for various landscape patterns. *Pattern recognition, 38*(12), 2626-2638. https://doi.org/10.1016/j.patcog.2005.05.009		2005
[AD23]	Hesselbarth, M.H.K., Sciaini, M., With, K.A., Wiegand, K., Nowosad, J. (2019). landscapemetrics: an open-source R tool to calculate landscape metrics. *Ecography, 42,* 1648-1657 (v2.1.1). https://r-spatialecology.github.io/landscapemetrics/		2019
[AD24]	Grimm, Mirco & Jones, Robert & Montanarella, Luca. (2002). Soil Erosion Risk in Europe.		2002

Ref.	Title	Version	Date
[AD25]	FAO and ITPS. 2015. Status of the World's Soil Resources (SWSR) – Main Report. Food and Agriculture Organization of the United Nations and Intergovernmental Technical Panel on Soils, Rome, Italy		2015
[AD26]	Poesen, J. (2018): Soil erosion in the Anthropocene: research needs. Earth Surface Processes and Landforms, 43(1): 64-84.		2018
[AD27]	Torri, D.; Poesen, J. (2014): A review of topographic threshold conditions for gully head development in different environments. In Earth Science Reviews, 130, pp. 73-85. DOI: 10.1016/j.earscirev.2013.12.006		2014
[AD28]	De Ploey, J. (1989): A Soil Erosion Map for Western Europe. Catena Verlag.		1989
[AD29]	Yassoglou, N., Montanarella, L., Govers, G., Van Lynden, G., Jones, R.J.A., Zdruli, P., Kirkby, M., Giordano, A., Le Bissonnais, Y., Daroussin, J. & King, D. (1998): Soil Erosion in Europe. European Soil Bureau.		1998
[AD30]	Morgan, R.P.C. (1995): Soil Erosion and Conservation. Second Edition. Longman, Essex.		1995
[AD31]	Montier, C., Daroussin, J., King, D. & Le Bissonnais, Y. (1998): Cartographie de l'aléa "Erosion des Sols" en France. INRA, Orléans.		1998
[AD32]	Wischmeier, W.H. & Smith, D.D. (1978). Predicting rainfall erosion losses – a guide for conservation planning. U.S. Department of Agriculture, Agriculture Handbook 537		1978
[AD33]	Renard, K.G., and Freimund, J.R. (1994). Using Monthly Precipitation to Estimate R-Factor in the Revised USLE. Journal of Hydrology, 127:287-306.		1994
[AD34]	Roose, E.J. (1977). Use of the Universal Soil Loss Equation to Predict Erosion in West Africa. In Soil erosion: Prediction and control. Soil Conservation Society of America, Special Publication no. 21. Ankeny, Iowa.		1977
[AD35]	Renard, K.G., Foster, G.R., Weessies, G.A., McCool, D.K., Yoder, D.C. (eds) (1997). Predicting Soil Erosion by Water: A guide to to conservation planning with the Revised Universal Soil Loss Equation (RUSLE). U.S. Department of Agriculture, Agriculture Handbook 703.		1997
[AD36]	Morgan, R.P.C., Morgan, D.D.V., Finney, H.J., 1984. A predictive model for the assessment of erosion risk. J. Agric. Eng. Res. 30, 245–253.		1984
[AD37]	Meyer, L.D., Wischmeier, W.H., 1969. Mathematical simulation of the process of soil erosion by water. Trans. Am. Soc. Agric. Eng. 12, 754–758.		1969
[AD38]	Morgan, R.P.C., 2001. A simple approach to soil loss prediction: a revised Morgan–Morgan–Finney model. Catena 44, 305–322.		2001
[AD39]	Laflen, J.M. & Elliot, William & Flanagan, Dennis & Meyer, C.R. & Nearing, Mark. (1997). WEPP-Predicting Water Erosion Using a Process-Based Model. Journal of Soil and Water Conservation. 52.		1997
[AD40]	J. C. Ascough II, C. Baffaut, M. A. Nearing, B. Y. Liu, 1997. The WEPP watershed model: I. Hydrology and erosion. Transactions of the ASAE. 40(4): 921-933. (doi: 10.13031/2013.21343)		1997
[AD41]	Kirkby, M.J., Irvine, B.J., Jones, R.J.A., Govers, G., Boer, M., Cerdan, O., Daroussin, J., Gobin, A., Grimm, M., Le Bissonnais, Y., Kosmas, C., Mantel, S., Puigdefabregas, J., Van Lynden, G., 2008. The PESERA coarse scale erosion model for Europe. I. — Model rationale and implementation. Eur. J. Soil Sci. 59, 1293–1306.		2008

Ref.	Title	Version	Date
[AD42]	Chandramohan, T., Venkatesh, B., and Balchand, A.N. (2015). Evaluation of Three Soil Erosion Models for Small Watershed. International Conference on Water Resources, Coastal and Ocean Engineering (ICWRCOE) Aquatic Procedia, 4:1227-1234.		2015
[AD43]	Desmet, P.J.J. & Govers, G. (1996). A GIS procedure for automatically calculating the USLE LS factor on topographically complex landcape units. Journal of soil and water conservation 51, p. 427-433.		1996
[AD44]	Lausch A, Erasmi S, King DJ, Magdon P, Heurich M. Understanding Forest Health with Remote Sensing -Part I—A Review of Spectral Traits, Processes and Remote-Sensing Characteristics. Remote Sensing. 2016; 8(12):1029. https://doi.org/10.3390/rs8121029		2016
[AD45]	Hansen MC, Potapov PV, Moore R, Hancher M, Turubanova SA, Tyukavina A, Thau D, Stehman SV, Goetz SJ, Loveland TR, Kommareddy A, Egorov A, Chini L, Justice CO, Townshend JR. High-resolution global maps of 21st-century forest cover change. Science. 2013 Nov 15;342(6160):850-3. doi: 10.1126/science.1244693		2013
[AD46]	Zolkos, S. G.; Goetz, S. J.; Dubayah, R. (2013): A meta-analysis of terrestrial aboveground biomass estimation using lidar remote sensing. In Remote Sensing of Environment 128 (4), pp. 289–298. DOI: 10.1016/j.rse.2012.10.017		2013
[AD47]	Winner, Hermann; Hakuli, Stephan; Lotz, Felix; Singer, Christina (2015): Handbuch Fahrerassistenzsysteme. Grundlagen, Komponenten und Systeme für aktive Sicherheit und Komfort / Hermann Winner, Stephan Hakuli, Felix Lotz, Christina Singer (Hrsg.). 3., überarbeitete und ergänzte Auflage. Wiesbaden: Springer Vieweg (ATZ/MTZ-Fachbuch).		2015
[AD48]	T. Vashum, Kuimi (2012): Methods to Estimate Above-Ground Biomass and Carbon Stock in Natural Forests - A Review. In J Ecosyst Ecogr 02 (04). DOI: 10.4172/2157-7625.1000116.		2012
[AD49]	Su, Yanjun; Guo, Qinghua (2014): A practical method for SRTM DEM correction over vegetated mountain areas. In ISPRS Journal of Photogrammetry and Remote Sensing 87 (21), pp. 216–228. DOI: 10.1016/j.isprsjprs.2013.11.009.		2014
[AD50]	Rosette, Jacqueline; Surez, Juan; Nelson, Ross; Los, Sietse; Cook, Bruce; North, Peter (2012): Lidar Remote Sensing for Biomass Assessment. In Lola Fatoyinbo (Ed.): Remote Sensing of Biomass - Principles and Applications: InTech.		2012
[AD51]	Rodríguez-Veiga, Pedro; Quegan, Shaun; Carreiras, Joao; Persson, Henrik J.; Fransson, Johan E.S.; Hoscilo, Agata et al. (2019): Forest biomass retrieval approaches from earth observation in different biomes. In International Journal of Applied Earth Observation and Geoinformation 77 (5), pp. 53–68. DOI: 10.1016/j.jag.2018.12.008.		2019
[AD52]	Pan, Yude; Birdsey, Richard A.; Fang, Jingyun; Houghton, Richard; Kauppi, Pekka E.; Kurz, Werner A. et al. (2011): A large and persistent carbon sink in the world's forests. In Science (New York, N.Y.) 333 (6045), pp. 988–993. DOI: 10.1126/science.1201609.		2011
[AD53]	Kumar, Lalit; Mutanga, Onisimo (2017): Remote Sensing of Above-Ground Biomass. In Remote Sensing 9 (9), p. 935. DOI: 10.3390/rs9090935.		2017

Ref.	Title	Version	Date
[AD54]	Hu, Tianyu; Su, Yanjun; Xue, Baolin; Liu, Jin; Zhao, Xiaoqian; Fang, Jingyun; Guo, Qinghua (2016): Mapping Global Forest Aboveground Biomass with Spaceborne LiDAR, Optical Imagery, and Forest Inventory Data. In Remote Sensing 8 (7), p. 565. DOI: 10.3390/rs8070565.		2016
[AD55]	Eggleston, H. S. (2006): 2006 IPCC guidelines for national greenhouse gas inventories. Hayama, Japan: Institute for Global Environmental Strategies.		2006
[AD56]	Choi, Yuyoung, Hye In Chung, Chul-Hee Lim, Jun-Hee Lee, Won Il Choi, and Seong Woo Jeon. 2021. "Multi-Model Approaches to the Spatialization of Tree Vitality Surveys: Constructing a National Tree Vitality Map" Forests 12, no. 8: 1009. https://doi.org/10.3390/f12081009		2021
[AD57]	Cherubini, P., Battipaglia, G. & Innes, J.L. Tree Vitality and Forest Health: Can Tree-Ring Stable Isotopes Be Used as Indicators?. Curr Forestry Rep 7, 69–80 (2021). https://doi.org/10.1007/s40725-021-00137-8		2021
[AD58]	Xulu, Sifiso & Peerbhay, Kabir & Gebreslasie, Michael. (2018). Remote sensing of forest health and vitality: a South African perspective. Southern Forests: a Journal of Forest Science. 81. 10.2989/20702620.2018.1512787.		2018
[AD59]	Dobbertin, M. Tree growth as indicator of tree vitality and of tree reaction to environmental stress: a review. Eur J Forest Res 124, 319–333 (2005). https://doi.org/10.1007/s10342-005-0085-3		2005
[AD60]	Larcher W (2001) Ökophysiologyie der Pflanzen. Ulmer Verlag, Stuttgart, 6. Auflage		2001
[AD61]	Gehrig, Martin: Methoden zur Vitalitätsbeurteilung von Bäumen: Vergleichende Untersuchungen mit visuellen, nadelanalytischen und bioelektrischen Verfahren, ETH Zurich, https://doi.org/10.3929/ETHZ-A-004685324, 2004.		2004
[AD62]	Hovi, A., Raitio, P., und Rautiainen, M.: A spectral analysis of 25 boreal tree species, Silva. Fennica, 51, 7753, https://doi.org/10.14214/sf.7753, 2017.		2017
[AD63]	Boyd, D. S. and Danson, F. M. (2005). Satellite remote sensing of forest resources: three decades of research development. Progress in Physical Geography 29, pp. 1–26.		2005
[AD64]	Huete, A. R.: Vegetation Indices, Remote Sensing and Forest Monitoring, Geography Compass, 6, 513–532, https://doi.org/10.1111/j.1749-8198.2012.00507.x, 2012.		2012
[AD65]	Tuominen, J., Lipping, T., Kuosmanen, V., and Haapane, R.: Remote Sensing of Forest Health, Geoscience and Remote Sensing, https://doi.org/10.5772/8283, 2009.		2009
[AD66]	Chuvieco, E.: Fundamentals of Satellite Remote Sensing : An Environmental Approach, CRC Press, Third Edition, https://doi.org/10.1201/9780429506482, 2020.		2020
[AD67]	Filella, I. und Penuelas, J.: The Red Edge Position and Shape as Indicators of Plant Chlorophyll Content, Biomass and Hydric Status, International Journal of Remote Sensing, 15, 1459–1470, https://doi.org/10.1080/01431169408954177, 1994.		1994
[AD68]	McDowell, N. G., Coops, N. C., Beck, P. S. A., Chambers, J. Q., Gangodagamage, C., Hicke, J. A., Huang, C., Kennedy, R., Krofcheck, D. J., Litvak, M., Meddens, A. J. H., Muss, J., Negrón-Juarez, R., Peng, C., Schwantes, A. M.,		2015

Ref.	Title	Version	Date
	Swenson, J. J., Vernon, L. J., Williams, A. P., Xu, C., Zhao, M., Running, S. W., and Allen, C. D.: Global satellite monitoring of climate-induced vegetation disturbances, Trends in Plant Science, 20, 114–123, https://doi.org/10.1016/j.tplants.2014.10.008, 2015.		
[AD69]	Stone, C. and Mohammed, C.: Application of Remote Sensing Technologies for Assessing Planted Forests Damaged by Insect Pests and Fungal Pathogens: a Review, Curr Forestry Rep, 3, 75–92, https://doi.org/10.1007/s40725-017-0056-1, 2017.		2017
[AD70]	Clark, M. L. und Roberts, D. A.: Species-Level Differences in Hyperspectral Metrics among Tropical Rainforest Trees as Determined by a Tree-Based Classifier, Remote Sensing, 4, 1820–1855, https://doi.org/10.3390/rs4061820, 2012.		2012
[AD71]	Rouse, J. W., Haas, R. H., Schell, J. A., und Deering, D. W.: Monitoring vegetation systems in the Great Plains with ERTS, NASA. Goddard Space Flight Center 3d ERTS-1 Symp., Vol. 1, Sect. A, 1974.		1974
[AD72]	Gnilke, A. and Sanders, T. G. M.: Distinguishing Abrupt and Gradual Forest Disturbances With MODIS-Based Phenological Anomaly Series, Front. Plant Sci., 13, https://doi.org/10.3389/fpls.2022.863116, 2022.		2022
[AD73]	Ahmad, S., Pandey, A. C., Kumar, A., Lele, N. V., and Bhattacharya, B. K.: Forest health estimation in Sholayar Reserve Forest, Kerala using AVIRIS-NG hyperspectral data, Spat. Inf. Res., 28, 25–38, https://doi.org/10.1007/s41324-019-00260-6, 2019.		2019
[AD74]	Verbesselt, J., Hyndman, R., Newnham, G., and Culvenor, D.: Detecting trend and seasonal changes in satellite image time series, Remote Sensing of Environment, 114, 106–115, https://doi.org/10.1016/j.rse.2009.08.014, 2010.		2010
[AD75]	Thonfeld, F., Hecheltjen, A., and Menz, G.: Bi-temporal Change Detection, Change Trajectories and Time Series Analysis for Forest Monitoring, pfg, 2015, 129–141, https://doi.org/10.1127/pfg/2015/0259, 2015.		2015
[AD76]	Ghaderpour, E. and Vujadinovic, T.: Change Detection within Remotely Sensed Satellite Image Time Series via Spectral Analysis, Remote Sensing, 12, 4001, https://doi.org/10.3390/rs12234001, 2020.		2020
[AD77]	Solberg, S., Næsset, E., Lange, H., & Bollandsa°s, O. M. (2004). Remote sensing of forest health. International Archives of Photogrammetry, Remote Sensing and Spatial Information Sciences, 36(Part 8), W2.		2004
[AD78]	Chávez, R. O., Estay, S. A., Lastra, J. A., Riquelme, C. G., Olea, M., Aguayo, J., and Decuyper, M.: npphen: An R-Package for Detecting and Mapping Extreme Vegetation Anomalies Based on Remotely Sensed Phenological Variability, Remote Sensing, 15, 73, https://doi.org/10.3390/rs15010073, 2022.		2022
[AD79]	Simoes, R., Camara, G., Queiroz, G., Souza, F., Andrade, P. R., Santos, L., Carvalho, A., and Ferreira, K.: Satellite Image Time Series Analysis for Big Earth Observation Data, Remote Sensing, 13, 2428, https://doi.org/10.3390/rs13132428, 2021.		2021

Ref.	Title	Version	Date
[AD80]	Bai, J., Perron, P., 2003. Computation and analysis of multiple structural change models. 470 Journal of Applied Econometrics 18 (1), 1–22. https://doi.org/10.1002/jae.659		2023
[AD81]	Fauvel, M., Chanussot, J., & Benediktsson, J. A. (2013). A spatial-spectral kernel-based approach for the classification of remote-sensing images. Pattern Recognition, 46(7), 1354-1365.		2013
[AD82]	Pal, M., & Mather, P. M. (2003). An assessment of the effectiveness of decision tree methods for land cover classification. Remote Sensing of Environment, 86(4), 554-565.		2003
[AD83]	Pettorelli, N., Vik, J. O., Mysterud, A., Gaillard, J. M., Tucker, C. J., & Stenseth, N. C. (2005). Using the satellite-derived NDVI to assess ecological responses to environmental change. Trends in Ecology & Evolution, 20(9), 503-510.		2005
[AD84]	Rodriguez-Galiano, V. F., Ghimire, B., Rogan, J., Chica-Olmo, M., & Rigol-Sanchez, J. P. (2012). An assessment of the effectiveness of a random forest classifier for land-cover classification. ISPRS Journal of Photogrammetry and Remote Sensing, 67, 93-104.		2012
[AD85]	Thenkabail, P. S., Enclona, E. A., Ashton, M. S., & Van Der Meer, B. (2004). Accuracy assessments of hyperspectral waveband performance for vegetation analysis applications. Remote Sensing of Environment, 91(3-4), 354-376.		2004
[AD86]	Zhu, X. X., Tuia, D., Mou, L., Xia, G. S., Zhang, L., Xu, F., & Fraundorfer, F. (2017). Deep learning in remote sensing: A comprehensive review and list of resources. IEEE Geoscience and Remote Sensing Magazine, 5(4), 8-36.		2017
[AD87]	Food and Agriculture Organization of the United Nations (FAO). (2020). The State of the World's Forests 2020. FAO.		2020
[AD88]	Grassi, G., House, J., Dentener, F., Federici, S., Den Elzen, M., & Penman, J. (2017). The key role of forests in meeting climate targets requires science for credible mitigation. Nature Climate Change, 7(3), 220-226.		2017
[AD89]	International Union for Conservation of Nature (IUCN). (2021). Bonn Challenge. IUCN.		2021
[AD90]	Dubayah, R., & Drake, J. B. (2000). Lidar remote sensing for forestry. Journal of Forestry, 98(6), 44-46.		2000
[AD91]	Townshend, J. R. G., & Justice, C. O. (1986). Analysis of the dynamics of African vegetation using the normalized difference vegetation index. International Journal of Remote Sensing, 7(11), 1435-1445.		1986
[AD92]	Lang, Nico, Walter Jetz, Konrad Schindler, and Jan Dirk Wegner. "A high-resolution canopy height model of the Earth." arXiv preprint arXiv:2204.08322 (2022).		2022
[AD93]	Abich, Amsalu, Mesele Negash, Asmamaw Alemu, and Temesgen Gashaw. 2022. "Aboveground Biomass Models in the Combretum-Terminalia Woodlands of Ethiopia: Testing Species and Site Variation Effects" Land 11, no. 6: 811. https://doi.org/10.3390/land11060811		2022

Ref.	Title	Version	Date
[AD94]	Friis, Ib & Demissew, Sebsebe & Breugel, Paulo. (2010). Atlas of the Potential Vegetation of Ethiopia. 58. 307.		2010
[AD95]	Chave, J., Réjou-Méchain, M., Búrquez, A., Chidumayo, E., Colgan, M.S., Delitti, W.B.C., Duque, A., Eid, T., Fearnside, P.M., Goodman, R.C., Henry, M., Martínez-Yrízar, A., Mugasha, W.A., Muller-Landau, H.C., Mencuccini, M., Nelson, B.W., Ngomanda, A., Nogueira, E.M., Ortiz-Malavassi, E., Pélissier, R., Ploton, P., Ryan, C.M., Saldarriaga, J.G. and Vieilledent, G. (2014), Improved allometric models to estimate the aboveground biomass of tropical trees. Glob Change Biol, 20: 3177-3190. https://doi.org/10.1111/gcb.12629		2014
[AD96]	Jucker, Tommaso & Fischer, Fabian & Chave, Jérôme & Coomes, David & Caspersen, John & Ali, Arshad & Loubota Panzou, Grace Jopaul & Feldpausch, Ted & Falster, Daniel & Usol'tsev, Vladimir & Adu-Bredu, Stephen & Alves, Luciana & Aminpour, Mohammad & Ilondea Bhely, Angoboy & Anten, Niels & Antin, Cécile & Askari, Yousef & Muñoz, Rodrigo & Narayanan, Ayyappan & Zavala, Miguel. (2022). Tallo: A global tree allometry and crown architecture database. Global change biology. 28. 10.1111/gcb.16302.		2022
[AD97]	Mugasha, Wilson & Mwakalukwa, Ezekiel & Luoga, E.J. & Malimbwi, R.E. & Zahabu, Eliakimu & Silayo, Dos Santos & Sola, Gael & Crete, Philippe & Henry, Matieu & Kashindye, Almas. (2016). Allometric Models for Estimating Tree Volume and Aboveground Biomass in Lowland Forests of Tanzania. International Journal of Forestry Research. 2016. 1-13. 10.1155/2016/8076271.		2016

Web References

Ref.	URL	Description	Last access
[URL01]	https://www.fao.org/sustainable-forests-management/en/#:~:text=The%20aim%20of%20sustainable%20forest,the%20sustainable%20development%20of%20communities	Description of aims of sustainable forest management.	2024/03/18
[URL02]	https://wwv.isa-arbor.com/education/onlineresources/dictionary	Definition of vitality by the International Society of Arboriculture	2024/03/18
[URL03]	https://sentinels.copernicus.eu/documents/247904/685211/Sentinel-2_User_Handbook.pdf/8869acdf-fd84-43ec-ae8c-3e80a436a16c?t=1438278087000	Sentinel 2 User Handbook	2024/03/18

1 Scope

This document consolidates the findings of our research efforts, benchmarking exercises, testing and algorithm selection processes leading up to the completion of Task 3: Algorithm Trade-off and Proof of Concept. The selected algorithms in this document will be further developed and integrated into a processing system on a cloud computing infrastructure (Task 4), applied in the national demonstrations (Task 5) and showcased in the Early Adopter Use Cases (Task 6). All methodological decisions presented here are informed by a solid review of EO best practices and scientific publications.

The thorough literature review is followed by algorithm experimental assessments and cross comparison of the best candidate methods over well selected test sites, which justify the algorithm choices.

2 Forest Mask (FM)

2.1 Theoretical background

Forest masks are a central tool for remote sensing related research. They are essential for the assessment and monitoring of forest areas and thus make an important contribution to environmental studies and the conservation of biodiversity in forests worldwide. Using these masks, valuable information on forest cover can be extracted from remote sensing imagery and provide a comprehensive understanding of forest dynamics at different spatial and temporal scales. Remote sensing technologies such as satellite and airborne sensors have revolutionized the way the Earth's ecosystems are monitored and managed. In this context, forest masks refer to binary classification maps that distinguish between forested and non-forested areas within a given geographic region. The creation of these masks requires the application of various image processing techniques and classification algorithms to remote sensing data such as multi-spectral and hyper-spectral imagery.

The theoretical basis of these forest masks is based on the principles of image interpretation and classification. Traditional methods used spectral signatures that relied on the unique reflectance properties of different land cover types. More recently, however, more sophisticated techniques have been incorporated, including machine learning algorithms such as Random Forests, Support Vector Machines and Convolutional Neural Networks, to improve the accuracy and efficiency of forest mask generation. A crucial aspect of development is the consideration of temporal dynamics. Because forests are subject to seasonal changes, the ability to capture these fluctuations is essential for a comprehensive understanding of forest ecosystems. In particular, the inclusion of time series analysis techniques and multi-temporal satellite imagery enables the creation of dynamic forest masks. These can be used to provide more precise insights into the phenology of forests, disturbance events and recovery processes. Studies have demonstrated the effectiveness of forest masks in applications ranging from carbon sequestration assessments to endangered species habitat monitoring. For example, in the work of Hansen et al. (2013) [AD45], forest masks derived from Landsat data were used to create a global forest change dataset that provides important information on deforestation and afforestation dynamics.

In summary, the theoretical basis of forest masks in remote sensing involves a combination of spectral analysis, image classification algorithms and temporal considerations. The integration of different data sources and advanced analysis techniques contributes to the accuracy and applicability of these masks in environmental research. As technology evolves, the refinement of forest mask methods will undoubtedly enhance our ability to monitor and manage forest ecosystems on a global scale, supporting sustainable development and conservation efforts.

Scientific Trade-Off Analysis

Remote sensing technology has led to a diversification of approaches for creating forest masks, each with its strengths and limitations, depending on factors like desired accuracy, computational resources, and data availability.

Spectral indices, such as the Normalized Difference Vegetation Index (NDVI), have been foundational in remote sensing applications for vegetation detection. Their simplicity and efficiency make them particularly attractive for large-scale applications, since they can be calculated on satellite data from Sentinel or Landsat. However, their effectiveness can be compromised under conditions of cloud cover or atmospheric particulates, which affect the spectral signatures of vegetation [AD83]. Furthermore, these methods may struggle with mixed pixel issues, where a single pixel contains multiple land cover types, which could lead to a significant reduced classification accuracy [AD85].

A different approach could be a supervised or unsupervised classification approach. Supervised classification techniques, including Random Forests and Support Vector Machines, rely on manual labeled training data to classify different land cover types. These methods have been praised for their flexibility and high accuracy in identifying various land cover types, including forests [AD82]. However, the requirement for substantial, accurately labelled training data and the computational demands of these algorithms can be significant barriers to their application, especially in resource-constrained settings [AD84]. Unsupervised classification algorithms like k-means clustering on the other hand do not rely on gathering training data, instead they have the function to automatically group pixels regarding their spectral properties. In spite of its usefulness, the accuracy of unsupervised classification does not always match actual land cover types, and expert interpretation is required to adjust cluster assignments to meaningful categories [AD81].

More recent approaches use the advent of machine learning or deep learning. Due to them, highly accurate methods for land cover classification were introduced, capable of handling complex and big scale datasets. Furthermore, they can improve over time when additional data is gathered [AD86]. These methods, however, demand extensive data for training accurate AI-models, which makes them quite time costly to develop. Another problem which may limit accessibility especially for some smaller projects could be the considerable computing resources required to process large amounts of data. However, since the availability of training data is steadily increasing with the growing number of research projects using AI-based methods, it can be assumed that AI-driven classification will become much more common in the future.

It can be concluded that all the approaches mentioned are suitable for creating forest masks. However, the accuracy of these is ultimately always determined by the availability of the required resources and the quality of the original data. In many cases, it can also be useful to combine the methods shown in order to further improve the results.

2.2 Proof of Concept

2.2.1 Methods selection

The method chosen for creating the basic forest mask of 2017 involves generating accurate forest area statistics for Ethiopia by calibrating Global Forest Change (GFC) map products with high-resolution RapidEye-based benchmark maps, which have an accuracy of at least 89%. This process includes the use of forest-type dependent calibrated thresholds of tree cover density, identified by assessing the potential vegetation of Ethiopia to classify three main forest types. The calibration process involved creating 100 GFC-based forest classifications using 1%-wise thresholds of tree cover percentage, followed by an accuracy assessment against the high-resolution maps based on 12,000 random points in test sites. The

optimal tree cover percentage thresholds were selected based on their fit and the balance between commission and omission errors. Finally, the GFC dataset for Ethiopia was refined by applying these thresholds, resulting in a calibrated forest map with a 30m spatial resolution for 2017, after correcting for forest gain and loss up to that year.

The process of updating the 2017 forest mask involved integrating various datasets to identify areas of forest gain and loss. Utilizing a canopy height dataset by Lang et al. (2022) [AD92], areas were marked as forest gain if tree heights exceeded 5 meters, where previously no forest was recorded. Further, the analysis included Sentinel-2 data to evaluate the Normalized Difference Vegetation Index (NDVI) trends, with specific thresholds set for determining forest gain and loss based on NDVI values. Only pixels meeting all criteria across the datasets were classified accordingly. The resultant forest gain and loss data were then applied to revise the initial forest mask, thus providing a refreshed forest classification for Ethiopia by 2020. However, the methodology faced uncertainties, particularly due to potential inaccuracies in canopy height measurements and NDVI trends, which could be affected by cloud coverage, thus introducing possible errors in the forest classification process.

2.2.2 Synthesis

Finally, an alternative method for creating a forest mask for 2017 was developed as part of this project. This method is based on the fact that a good data basis was already available with the forest mask by Hansen et al. (2013) [AD54], which could be further improved by the selected calibration process. The availability of high-resolution data was another deciding factor in the choice of process. For the update to 2020, the vegetation index-dependent process was also integrated into the forest mask. The combined method has already been applied in the entire Ethiopian study area as well as in the individual sub-study areas. Satisfactory results were achieved in initial qualitative comparisons.

2.3 Final Specification of EO solution

In order to produce an updated forest mask, the user needs the calibrated forest mask from 2017, a shapefile of the area of interest and Sentinel-2 time-series data. The user defines the desired year for which the updated forest mask should be produced and calculates the maximum NDVI and the change between the time steps of the old and new forest mask based on Sentinel 2 data. The CHM layer from Lang et al. (2022) [AD92], which is required for the growth of the forest, is already implemented and hosted on the platform and does not need to be loaded separately. This is further described under 5.3.1 in this document.

Involving CHM, the NDVI maximum and the NDVI, the algorithm then classifies the AOI according to the following pixel value criteria (Table 1):

Table 1. Categorisation of forest loss and gain for FM

Forest loss	Forest gain
NDVI change t0-t1 < -0.15 Inside of 2017 Forest Mask	NDVI change t0-t1 > 0.3 NDVImax > 0.6 Tree height > 5m Outside of 2017 Forest Mask

Unaffected forest area will stay classified as forest.

The output file will be an 10m resolution raster of forest and non-forest (Figure 1, Figure 2).

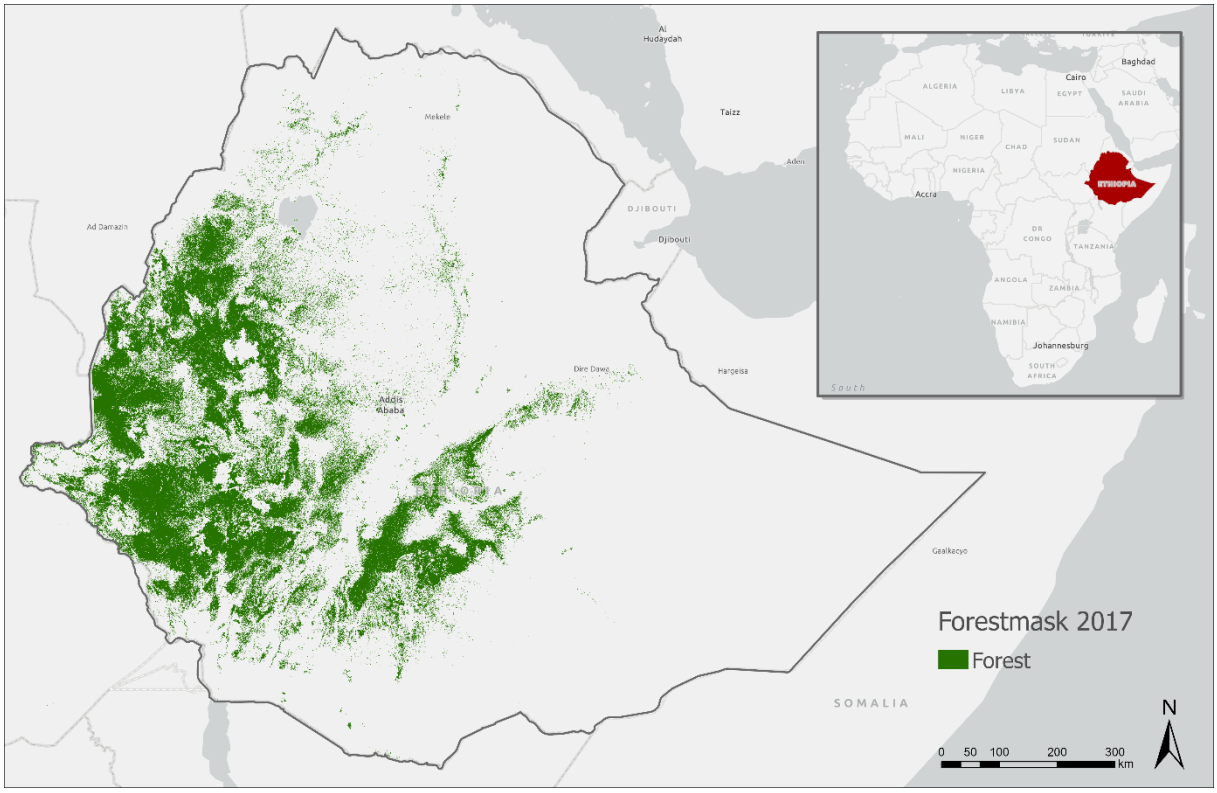

Figure 1. Result forest cover 2017

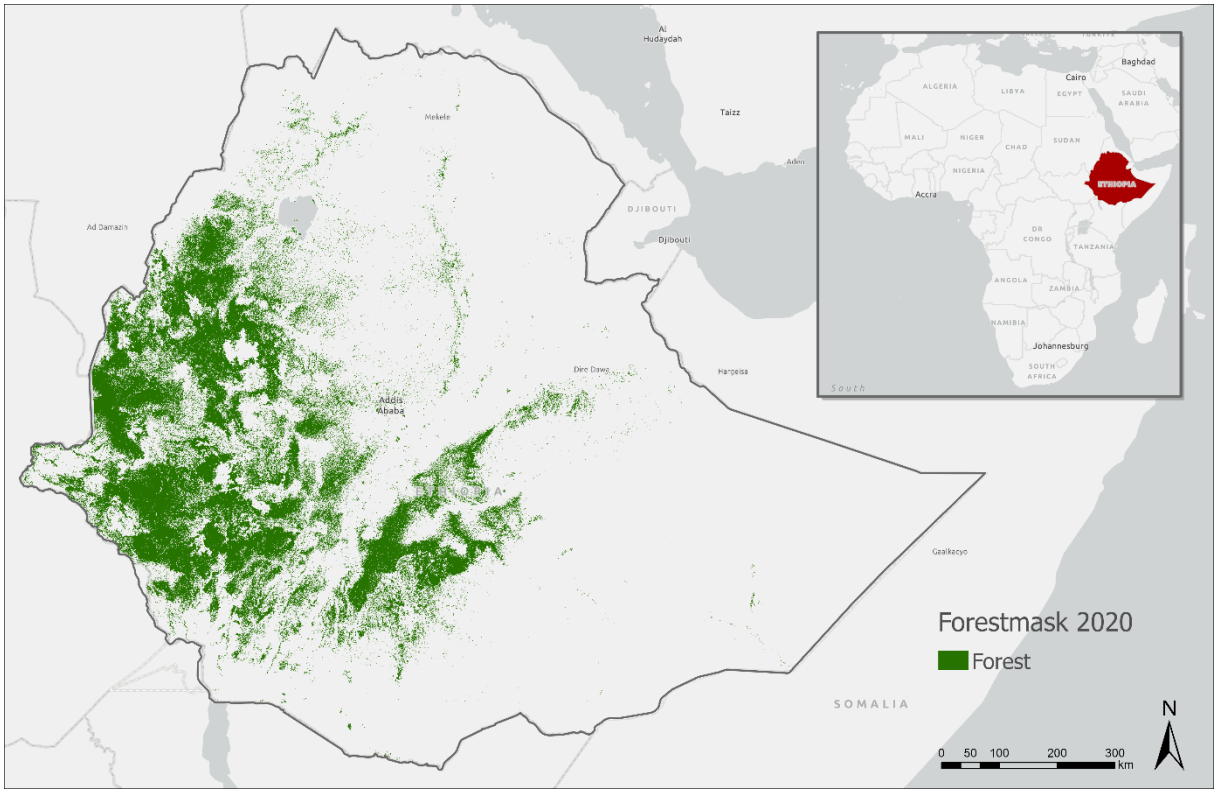

Figure 2. Result forest cover 2020

3 Forest Area Net Change Rate (FNC)

3.1 Theoretical background

In general terms, the forest area net change rate refers to the total change in the amount of forested land over a given period of time. It is usually expressed as a percentage and reflects the balance between processes such as deforestation, afforestation, reforestation and natural disturbances within a given geographical forest region.

Deforestation refers to the permanent removal of forests to make the land available for other uses, such as agriculture, urban development, or mining. This process has profound ecological impacts, including loss of biodiversity, disruption of water cycles, soil erosion, and contributing significantly to climate change through the release of stored carbon dioxide. According to the Food and Agriculture Organization of the United Nations (FAO), approximately 10 million hectares of forest are lost annually, a rate that underscores the urgent need for global conservation and sustainable land use practices [AD87].

Reforestation on the other hand, involves replanting trees in areas where forests have been cut down or destroyed, usually with the aim of restoring the original forest cover. Reforestation can be natural, where the forest regenerates itself over time, or active, involving the deliberate planting of trees. It helps in rebuilding habitats, restoring biodiversity, and enhancing ecosystem services such as water regulation, soil protection, and carbon storage. Research indicates that reforestation can significantly contribute to the global carbon budget, offering a vital lever for climate change mitigation [AD88].

While afforestation addresses the process of planting trees on lands that have not been forested for at least 50 years. It serves as a strategic tool for carbon sequestration, enhancing biodiversity, and restoring degraded lands. Afforestation efforts can mitigate the effects of deforestation and climate change by absorbing CO2 from the atmosphere, thus playing a crucial role in achieving the goals set by the Paris Agreement to combat climate change. For instance, the "Bonn Challenge" aims to restore 350 million hectares of degraded and deforested lands by 2030, highlighting the global commitment to afforestation and reforestation initiatives [AD89].

Deforestation primarily contributes to climate change and environmental degradation, afforestation and reforestation represent hopeful strategies for ecological restoration and climate mitigation. Efforts to combat deforestation, promote afforestation, and facilitate reforestation are integral to achieving the United Nations Sustainable Development Goals (SDGs), particularly those related to life on land (SDG 15), climate action (SDG 13), and sustainable cities and communities (SDG 11). The FNC metric provides insight into the condition and sustainability of forest ecosystems. It therefore serves as a key indicator for environmental assessments and continuous monitoring allows an understanding of the impact of human activities and natural processes on global forest cover to be inferred.

Scientific Trade-Off Analysis

In principle, the methods used for the FNC overlap strongly with the methods used for the forest mask. In order to be able to determine forest growth or loss, a clearly defined section of a forest area is required from which changes can be recorded.

Therefore, in principle, the methods already mentioned can be used to create forest masks in order to ultimately classify several forest areas over the desired time period. By directly comparing these areas in a time-series analysis, statements can then be made about forest loss and forest gain.

The basic approach for tracking would therefore be to keep track of NDVI changes. This method allows for the effective monitoring of changes over time, highlighting areas of deforestation or reforestation. Applications of NDVI in forest management include detecting illegal logging activities, assessing the impacts of climate change on forest ecosystems, and evaluating reforestation efforts. Studies have

shown that NDVI is particularly effective in tropical forests, where the dense canopy and diverse ecosystems present unique monitoring challenges [AD83, AD91]. In general, however, it should be noted that NDVI calculations, as already mentioned, can be susceptible to disturbances such as cloud cover and therefore data quality must always be taken into account.

Another approach can be the use of Light Detection and Ranging (LIDAR) systems. LIDAR systems, by emitting pulses of laser light and measuring the time they take to return after hitting the surface, provide precise three-dimensional information about forest structure, including canopy height, biomass, and even ground-level characteristics under dense canopy cover [AD90]. The height information obtained in this way can then be used as Canopy Height Model (CHM) in a time comparison to make statements about the disappearance or growth of forest in the observation area. However, similar to the use of remote sensing data to determine the NDVI, the method is susceptible to interference from clouds. In addition, atmospheric haze can attenuate the signal before it reaches the ground, leading to inaccuracies in the information.

Another aspect is that high-resolution LIDAR measurements are very expensive and are therefore hardly available for larger areas.

Both methods mentioned can be used to recognise changes in forest areas. However, it is always necessary to weigh up which data is available in which context and in which quality and whether it is not more practical to combine the methods in the selected project. This could compensate for mutual weaknesses and improve the final result.

3.2 Proof of Concept

3.2.1 Methods selection

The methodology employed to assess FNC involves a comprehensive approach that integrates various datasets to quantify forest gains and losses between distinct forest classifications or across temporal intervals. This process adheres to an updated forest mask methodology, deploying two divergent techniques to delineate forest dynamics accurately. To determine forest gains, the method incorporates three distinct datasets: a global canopy height dataset to assess tree heights, yearly maximum NDVI trends derived from Sentinel-2 data, and an additional NDVI layer from a specific year. Forest gain is identified through a composite analysis where specific criteria across all three datasets must be met, and this gain is then isolated to areas previously non-forested as of a baseline year. Conversely, forest loss is detected through analysis of negative NDVI trends, with losses classified within the confines of the initial forest mask to accurately represent net changes.

3.2.2 Synthesis

There are various ways to determine forest loss or growth. In particular, vegetation indices and canopy height data can provide sources of information for the Forest Area Net Change Rate of change of forest area. This project attempts to increase the accuracy of the final product by using combined approaches. However, this requires certain data to be available. In order to be able to distinguish the increment outside the forest areas over time, it is necessary that a forest mask is available. It is also necessary that a CHM of the relevant study area is available. If this is the case, results can be obtained quickly with this method, even in large study areas.

Though this process can be subject to uncertainties, notably in canopy height measurements and NDVI values potentially affected by cloud cover, which may introduce classification errors.

3.3 Final Specification of EO solution

To calculate the FNC, the user must provide an area of interest (AOI) and a forest mask that represents the forest areas within the study area before the change. The mask must be available as a shapefile. The AOI can either be defined as a polygon selection on the platform itself or also imported as a shapefile.

The CHM layer from Lang et al. (2022) [AD92], which is required for the growth of the forest, is already implemented and hosted on the platform and does not need to be loaded separately.

The user defines the desired time period in which the FNC calculates the maximum NDVI and the change between the time periods from Sentinel 2 data. Further described under 5.3.1. In this document.

Involving CHM, the NDVI maximum and the NDVI, the algorithm then classifies the AOI according to the following pixel value criteria (Table 2):

Table 2. Categorisation of forest loss and gain for FNC

Forest loss	Forest gains
NDVI change t0-t1 < -0.15 Inside of 2017 Forest Mask	NDVI change t0-t1 > 0.3 NDVImax > 0.6 Tree height > 5m Outside of 2017 Forest Mask

Unaffected forest area will stay classified as forest.

The output file will be an 10m resolution raster, including a class value for forest gain, forest loss and forest area unchanged (Figure 3).

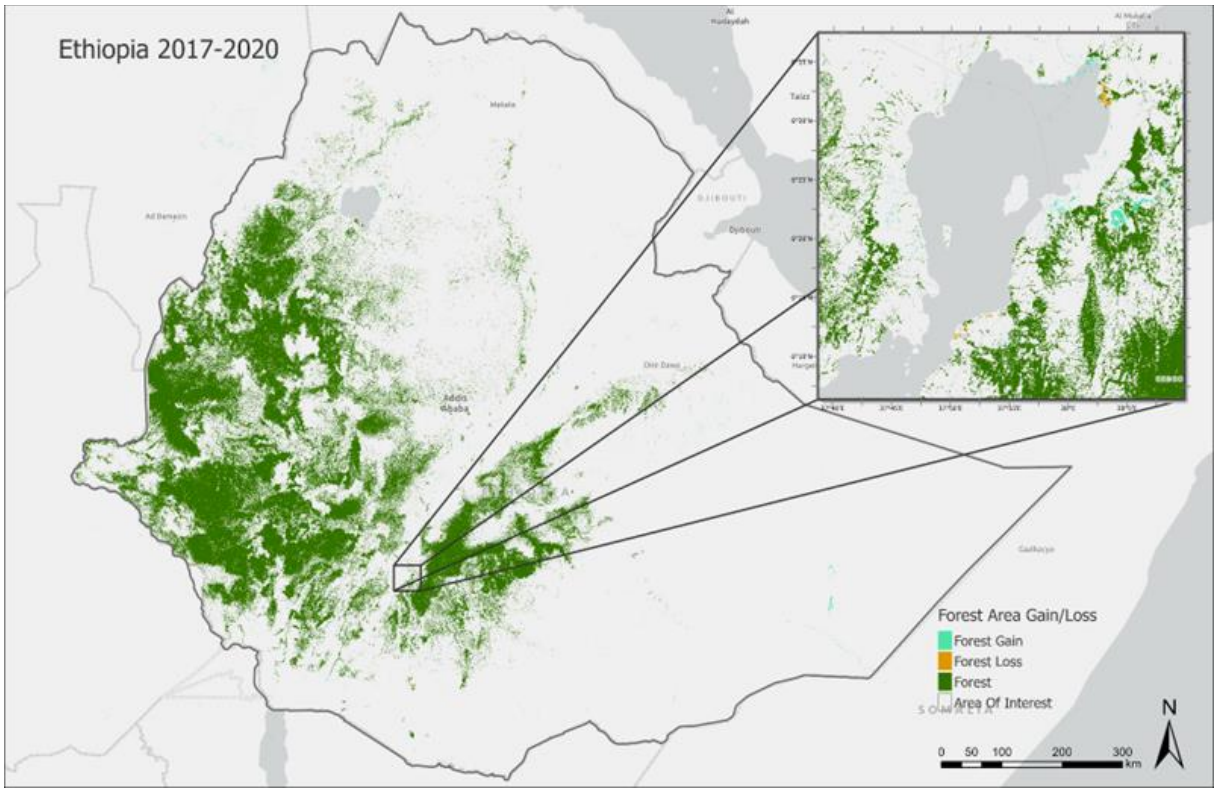

Figure 3: Visualisation of FNC for Ethiopia, 2017-2020

4 Above-Ground Biomass Stock (AGB)

4.1 Theoretical background

Biomass is vital for the removal of carbon dioxide (CO2) from the atmosphere, predominantly through the processes of photosynthesis and respiration. It encompasses the above-ground and below-ground components of plant life, playing a significant role in the exchange of large quantities of CO2 between the atmosphere and terrestrial ecosystems [AD55]. According to Pan et al. (2011) [AD52], it is estimated that the world's forests store about 861 gigatons of carbon - 44 percent in the soil (up to one meter deep), 42 percent in living above-ground and below-ground biomass, 8 percent in dead wood, and 5 percent in litter [AD52].

In the last decades the carbon dioxide concentration in the Earth's atmosphere has been steadily increasing due to human activities, such as burning fossil fuels and deforestation. This rise in carbon dioxide levels has disrupted the natural carbon cycle and contributed to global climate change. As mentioned before, especially forest ecosystems play a vital role in the carbon cycle by absorbing carbon dioxide. Tropical forests, in particular, act as significant carbon reservoirs. Estimating forest carbon stocks is therefore not just only crucial for the understanding of carbon exchange between forests and the atmosphere but also for the assessment of impacts of deforestation and forest degradation along with the prediction of future changes in carbon stocks. It is additionally helpful for the development of new sustainable forestry planning methods.

In order to estimate the carbon stock of forests, researchers tend to take a look at the forest above ground biomass (AGB). Accurately estimating forest biomass is crucial for assessing forest productivity, sustainability, and carbon emissions. It provides insights into the amount of carbon that can be released when forests are cleared or burned. Biomass estimation helps to understand the potential carbon sequestration capacity of forests. It is essential for various applications, including timber extraction, monitoring changes in carbon stocks, and understanding the global carbon cycle [AD48].

Scientific Trade-Off Analysis

Estimating forest biomass can be done through various methods, where field measurements and remote sensing-based methods play a large role. With field measurements the AGB can be assessed through both destructive and non-destructive methods. The destructive approach, known as the harvest method, involves cutting down and weighing trees. This method is often used in areas with uniform tree sizes, such as pine plantations, and estimates are extrapolated based on a selected sample. However, the harvest method has limitations due to its destructive nature, time-consuming process, high costs, and potential impact on endangered plants and animals. Non-destructive methods offer alternative approaches, such as using allometric equations. Allometric equations utilize tree measurements like diameter at breast height (dbh) and height, although they are more applicable in homogeneous forests or plantations with similar-aged stands. These equations may have limited utility in heterogeneous forests where tree characteristics vary significantly [AD53].

In addition to field measurements, technologies from earth observation (EO) are being used for biomass determination. EO methods not only yield the advantage of covering large areas but also the possibility of monitoring poorly accessible regions of interest. There are three main remote sensing-based approaches for biomass estimations based on different input datasets, namely light detection and ranging (LiDAR), Radar (SAR)- and optical remote sensing data [AD54].

LiDAR is an optical technique used to determine the position and distance of objects in space. It operates on a similar principle to radar, but instead of microwaves, LiDAR utilizes beams of ultraviolet, infrared, or visible light [AD47]. Using these focused short-wavelength laser pulses, LiDAR sensors are able to penetrate the forest canopy in a more effective way then than other systems [AD49]. This allows direct

and more accurate measurements of canopy structure variables, such as canopy height distributions, which are needed for AGB estimations. However, the use of LiDAR at a national scale is often not feasible due to its disadvantage in temporal and spatial coverage. As of now, global continuity in LiDAR measurements has been challenging to achieve due to the constraints of both airborne LiDAR and spaceborne LiDAR platforms. Airborne LiDAR data is only available in select small regions, primarily due to the high costs involved in conducting airborne LiDAR flight missions [AD46]. In the future LiDAR may have the potential of becoming a low-cost alternative at lower spatial resolution.

Another possible approach is a radar (SAR)-based biomass assessment, whereby the backscatter from radar-satellites is directly correlated to in-field estimated biomass values. Microwave active sensors, such as SAR, provide valuable information about the dielectric and structural properties of objects, soil surfaces, and plants. One key advantage of microwave radar sensors is their ability to penetrate through clouds, making them weather and daytime independent and enabling image acquisitions in even the cloudiest regions on Earth. This feature sets radar imagery apart from optical imagery, which can be hindered by cloud interference [AD51]. This approach however is not suitable for all forest types and depends also on the type of the radar data.

A final approach is using canopy height information that can be derived from airborne or even spaceborne data, since the height of trees is often correlated to the biomass of trees. In contrast to these active sensors, passive sensors can also be used to estimate biomass. Passive remote sensors are able to measure different wavelengths of reflected solar radiation. In doing so, they provide two-dimensional information that indirectly relates to biophysical properties of the vegetation [AD50].

In all cases, sufficient, i.e., qualitatively and quantitatively adequate, data from local forest inventories are needed as the with the aforementioned methods captured parameters, such as tree height, need to be calibrated by linking ground measurements with remotely sensed data [AD54]. Therefore, these techniques cannot directly acquire AGB estimations. The better the field data and the better the EO data, the higher the TIER level and thus the higher the accuracy of the biomass estimate can be.

4.2 Proof of Concept

4.2.1 Methods selection

Due to the complexity of the biomass calculation, the product method is based on a combination of freely available field inventory data from open source databases and remote sensing data as well as the availability of allometric equations from our own previous research at RSS and scientific publications (Figure 4).

First, a land cover classification was used to divide the forest classes into different biomes. For each of these forest biomes, all available information on tree species was collected from the scientific literature. The tree species were then checked for their availability in an open-source tree database and their biomass-relevant properties were extracted. Regression analyses were then carried out between tree height and breast height diameter. The resulting reference equations were then used in the biome-specific AGB allometry to calculate an average biomass estimation for the study areas using a global surface height model.

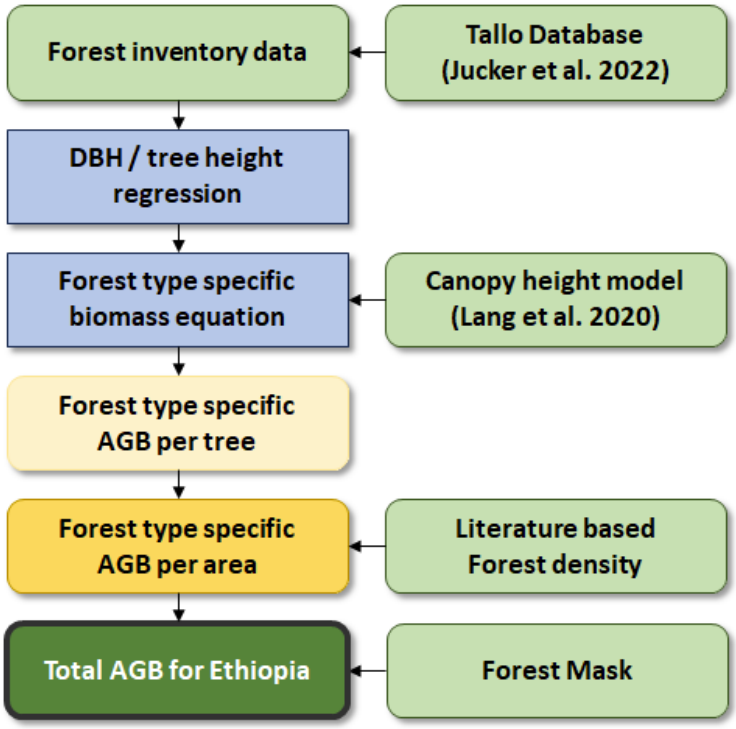

Figure 4. AGB-Product workflow chart

4.2.2 Synthesis

As already mentioned, estimating biomass is a major challenge. The complexity of the chosen method reflects this. In order to obtain a meaningful final result, a lot of time must be invested in literature research. The method is also heavily dependent on freely available tree inventory data, which is required as a key input. In addition, allometries calibrated using local trees are also available for selected tree types. Finally, the timeliness of the results always depends on the date of the selected CHM. The method has already been applied to the entire study area in Ethiopia and shows valid results in initial qualitative comparisons with other large-scale biomass estimates. However, automated implementation within the scope of this project is proving difficult due to the complexity and labour required.

4.2.3 Final Specification of EO solution

In principle, a large number of different input types are required for processing.

The respective biome types are first imported with the help of a vegetation classification by Friis et al. (2010) [AD94] which was read in as a vector file.

For the relevant characteristics (diameter at breast height, height) of the biomimetic tree species, the Tallo database by Jucker et al. (2022) [AD96] is used. This is used to determine the regression analyses between diameter at breast height and height, which are inserted into the respective biomass allometries.

For the calculation, biomass allometries were determined for each biome based on a literature search.

Moist Afromontane Forest [AD95].:

$$AGB = 0.0673 * (WD * DBH^2 * H)^{0.976}$$

Dry Afromontane Forest [AD97]:

$$AGB = 0.1014 * (WD * DBH^2 * H)^{0.9510}$$

Combretum-Terminalia Woodland, Acacia-Commiphora Bushland [AD93]:

$$AGB = 0.0763 * (DBH^{2.2046} * H)^{0.4918}$$

The aforementioned canopy height layer with a resolution of 10 metres serves as the basic geodata for the following calculation in the algorithm.

The product must then be covered with a forest mask and multiplied by literature-based tree density values.

The final output raster shows an estimate of the biomass in tonnes/ha per pixel (Figure 5). The pixel resolution is based on that of the CHM by Lang et al. (2022) [AD92] and is therefore 10m.

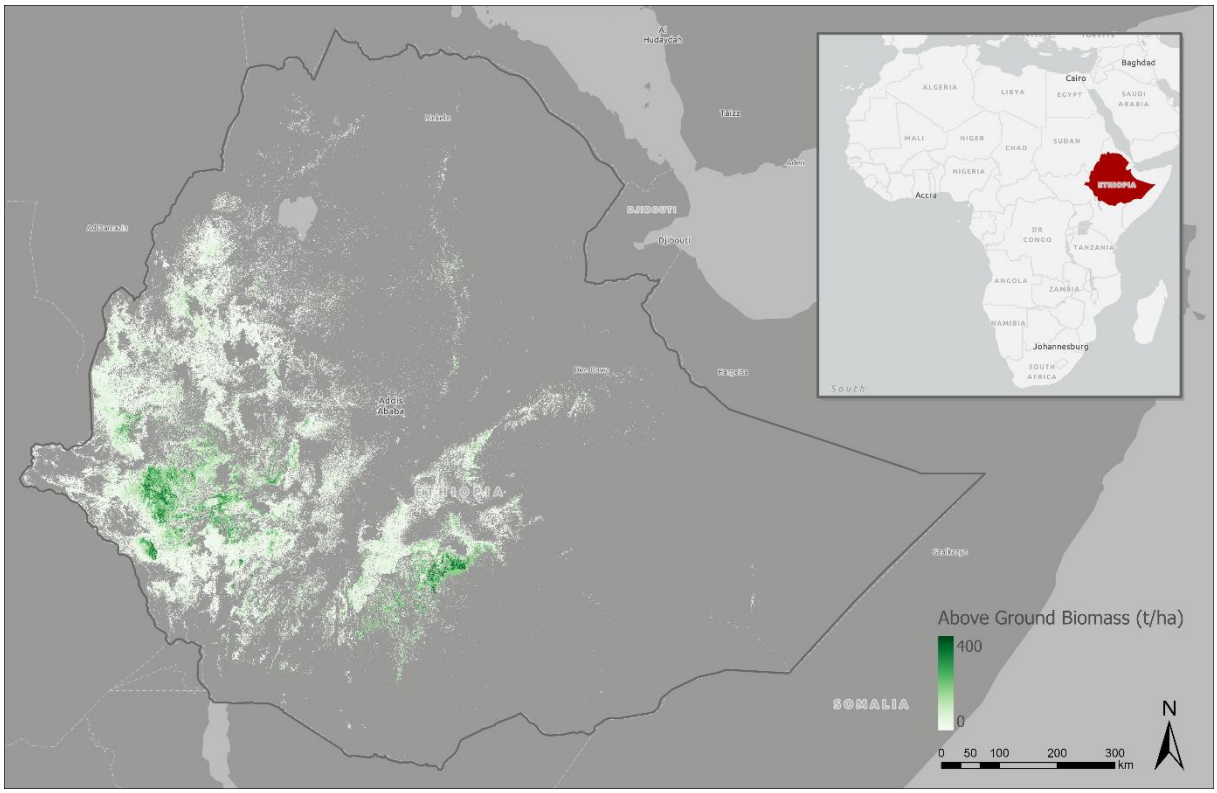

Figure 5. Final AGB-Estimation, 2020

5 Forest Condition Monitoring (FCM)

5.1 Theoretical background

The aim of sustainable forest management (SFM) is to ensure that forests supply goods and services to meet both present-day and future needs and contribute to the sustainable development of communities. One of the key elements of SFM is forest health and vitality [URL01]. The term "forest condition" comprises not only vitality but also forest damage or disturbance and thus represents a combination of both. To effectively maintain and improve forest condition, long-term forest monitoring is crucial to understand past, current and future forest condition dynamics [AD56].

Forest ecosystems are facing increasing anthropogenic pressures and disturbances at different scales, from local to global. In particular, the climate-induced increase in droughts is contributing to high levels of stress on forest stands worldwide, making them more susceptible to disease and parasites. As these challenges continue to increase, traditional terrestrial in situ monitoring approaches for forest ecosystems have made significant progress. However, they often rely on both labor-intensive methods and, in some cases, subjective indicators to assess forest health. Especially in remote areas, these methods are labour intensive and costly. In response to these limitations, remote sensing has emerged as a powerful tool for assessing forest health, enabling researchers and resource managers to collect valuable data over large areas efficiently. It can often offer a transformative solution that can bridge gaps by providing the ability to monitor forest health indicators at different spatial and temporal scales in a more frequent and cost-effective way. Satellite remote sensing provides a comprehensive and non-invasive method for monitoring forest conditions. The Sensors aboard satellites capture data across different wavelengths, allowing for the extraction of valuable information about various aspects of forests, such as vegetation health, biomass, and land cover changes. Spectral bands sensitive to chlorophyll content, water stress, and other indicators are particularly useful in assessing the overall health of forested areas.

According to Lausch et al. (2016) [AD44], the ability to monitor forest health indicators with remote sensing data depends on several factors. Both on the characteristics of forest features and their shape, density and distribution in space and time, as well as on the spatial, spectral, radiometric, angular and temporal resolution of RS sensors or multi-sensor systems. The choice of modelling technique (classification or estimation of biophysical/chemical variables) and entity representation (pixel-based or (geographically) object-based) also plays a role. And finally, how well the RS algorithm and its assumptions fit the remote sensing data and the plant characteristics and trait variations in forest ecosystems.

One of the most common approaches to monitor forest health is the vegetation indices (VIs) based approach. It involves the use of specific mathematical combinations of spectral bands, which can be obtained free of charge from Sentinel-2 data, to obtain meaningful information about the condition and characteristics of vegetation. One of the most used and most basic vegetation indices is the Normalized Difference Vegetation Index (NDVI). The NDVI is calculated as the normalized difference between the near infrared (NIR) and red (RED) reflectance values and provides a quantitative measure of the amount and strength of green vegetation. NDVI values range from -1 to +1, with higher values indicating healthier and more lush vegetation. The Enhanced Vegetation Index (EVI) is another vegetation index that addresses some of the limitations of NDVI, particularly in areas with dense vegetation or in the presence of atmospheric influences. EVI incorporates additional spectral bands and atmospheric correction, resulting in a more robust indicator of vegetation health. These methods can also be combined very well with time series data. This allows researchers to observe both positive and negative changes in forest health over long periods of time.

This is beneficial as monitoring forest health is a crucial aspect of achieving the Sustainable Development Goals (SDGs), as it impacts several key aspects of sustainable development in different ways. Firstly, forests are crucial for SDG 13 (climate action) as they serve as carbon sinks and thus make an important contribution to climate change mitigation. Monitoring the state of forests enables the assessment of carbon sequestration, deforestation rates and the state of ecosystems and provides important data for sound climate change mitigation strategies. In addition, SDG 15 (Life on Land) is closely linked to forest health monitoring, as forests harbour biodiversity, support ecosystems and contribute to the conservation of endangered species. Therefore, monitoring allows potential threats to biodiversity to be identified so that timely action can be taken. In addition, sustainable forest management practices that rely on monitoring are in line with SDG 12 (Responsible Consumption and Production) as they promote the sustainable use of terrestrial ecosystems. In essence, forest health monitoring becomes a linchpin for the interlinked SDGs and plays a crucial role in combating climate change, conserving biodiversity and promoting sustainable use of forest ecosystems.

5.1.1 Vitality

To date, there is still no clear and universally agreed definition or conception of forest vitality or forest health [AD57, AD58]. There can be found several definitions for vitality in the literature [AD59]. One example comes from the International Society of Arboriculture (ISA), where vitality is the overall health and ability of a plant to deal effectively with stress [URL02]. The vitality of a plant is a theoretical concept and cannot be measured directly. The optimal or maximum tree vitality is not known. Only the minimum vitality of a plant, when it is dead can be determined clearly in most cases. Consequently, only relative changes of suitable indicators can be measured to observe tree vitality. This vitality principle is schematically represented in Figure 6 for different stress cases [AD59].

Vitality is contingent on stress. Assessing the effects of external stress is important since it's an important criterion in most vitality concepts. Stress is defined as a significant deviation from the optimal condition for life. The longer the stress lasts, the weaker the vitality becomes [AD60]. The plant reacts to stress with increased efforts to repair damage (Figure 6, Case 1-3). After this action usually a recovery phase follows (Figure 6, Case 1 and 2). When stress is prolonged, the plant´s ability to cope with or to survive further stress decreases and the vitality declines (Figure 6, Case 2 b). Once a certain point is exceeded, irreversible damage occurs or the plant dies (Figure 6, Case 3) [AD59].

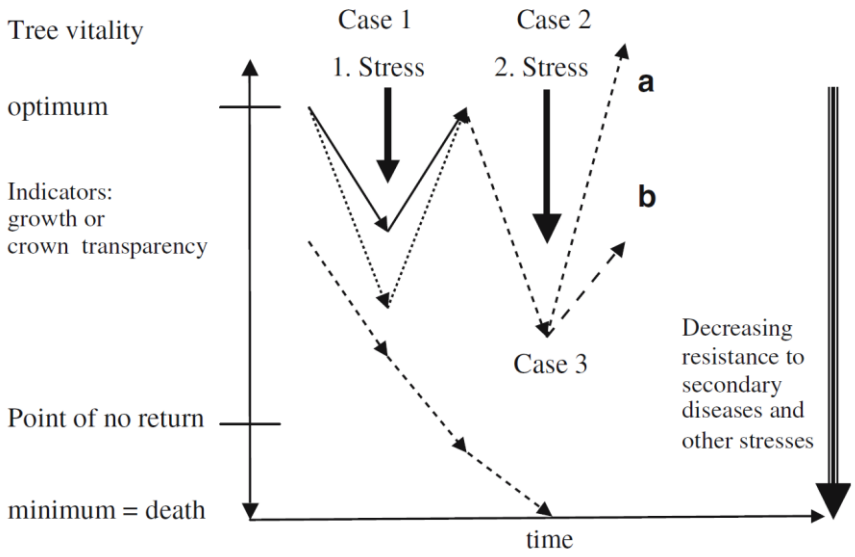

Figure 6. Tree vitality schema with the impact of stress [AD59]

To assess forest vitality informative and cost-effective methods to measure objective indicators are needed. The indicators should be suitable to capture the symptoms of deteriorated forest health. Forest vitality can be assessed on different levels.

At the plant cell level biochemical indicators like phytohormones or enzymes may best reflect the response of trees to different stressors [AD60]. But since these indicators cannot be collected for large areas and are very costly, they are not suitable for monitoring the vitality of a forest.

Field surveys are of great importance and a well-established approach for data collection in forest monitoring. The challenge in field measurements is to measure a suitable vitality indicator and the intensity and duration of the stress influence. Examples for common vitality indicators in field studies are crown foliage, growth in height, diameter or volume and leaf properties such as photosynthesis and nutrients

[AD59, AD61]. Since the conventional methods of collecting such data in the field are costly, difficult, partly subjective and on a smaller scale, there is a need for a more appropriate approach to monitor large forest areas [AD58].

This is where EO methods come into play, as they are the only practicable time- and cost-efficient technology for monitoring forest vitality for extensive and inaccessible regions and on a timely and consistent basis [AD62, AD63, AD64]. This data can be related to field observations, which is still essential for ground validation [AD57]. Many studies demonstrated the suitability of remote sensing data to monitor forest health [AD57, AD58]. Various types of airborne and satellite-based sensors such as photographs, multi- and hyperspectral images, radar and lidar have been used for this purpose [AD65].

Recent sensors like Sentinel-2 are suitable for forest vitality monitoring since it collects multispectral data in a high temporal and spatial resolution with global coverage. Sentinel-2 provides 10 suited spectral bands covering the visible to the short-wave infrared (SWIR) spectrum (490 nm - 2190 nm) [URL03]. Measuring the spectral signature of plants give insights in their biochemical, physical and physiological properties. The spectral signature of a plant is primarily defined by its biochemical components like pigments, lignins and water content. In the optical range of the spectrum the reflected radiation is primarily influenced by the pigments. In the red edge region, leaf pigments and cellulose become increasingly transparent for wavelengths of the NIR [AD66]. The red edge is also particularly useful for drawing conclusions about chlorophyll content, which is a good indicator of photosynthetic activity, nutrient availability and the developmental stage of the vegetation [AD67]. In the near infrared (NIR) range of the spectrum the vegetation reflectance is influenced by its morphology. The SWIR wavelengths are sensitive to the water content of the vegetation. Physiological properties of vegetation are reflected in its vitality, phenology and stress level and depend on the local availability of nutrients, water and light. By measuring the spectral reflectance, conclusions can be drawn in this respect. Since remote sensing sensors collect data from a nadir perspective, the tree crown and its canopy are in focus [AD66, AD68]. As the effects of stress are often reflected by changes in tree crown condition, the crown characteristics are considered good indicators of tree health [AD69].

To improve the detection of the vegetation signal, so-called vegetation indices (VI) have been developed and are used to estimate biophysical forest properties [AD64]. VI are simple, robust and well-researched techniques for quantitatively extracting vegetation quantity and vitality from multispectral remote sensing data [AD64, AD66]. Vegetation has a characteristic spectral behaviour with a high contrast between the red and NIR spectral regions. As a rule, the stronger this difference, the higher the amount and vitality of the vegetation. When vegetation senesces, the reflection in the NIR decreases and increases in the red wavelength range, which is why the difference and thus the VI value decreases [AD66]. To isolate or amplify the vegetation signal and minimise non-vegetation influences, typically at least two spectral bands of these wavelengths are combined for VI calculation [AD66, AD70]. Based on these spectral ratios, the first VI were developed as simple ratio-based indices, such as the widely used "Normalized Difference Vegetation Index" (NDVI) [AD71]. Table 3 gives an overview of the most important multispectral VI. Each VI is intended to highlight a particular vegetation property. For this purpose, VI are developed using empirical laboratory measurements of this property and correlation analyses with remote sensing data [AD65].

5.1.2 Disturbance

The global forest health is declining, with the main drivers being climate change, air pollution and increasing human activities [AD65]. These drivers led to increased rate of vegetation disturbances and mortality across all biomes and plant functional types on all vegetated continents. For this reason, large-scale condition monitoring is particularly important to understand changes in the condition of forest ecosystems [AD68].

There is no single definition for a disturbance that satisfies all scientific and societal questions, but it can be described as a negative deviation from the long-term phenology and thus a decrease in vitality [AD68, AD72]. Disturbances are an integral part in forest ecosystems, influencing the stand structure and regeneration [AD72]. Plants are regularly exposed to stress, as these site-bound organisms are dependent on a variety of environmental influences and stressors. Next to abiotic stressors such as air pollution, droughts, fires, floods and storms, biotic stressors like pathogens, insects and invasive species and anthropogenic causes such as pollution and deforestation place strain on the vegetation and can cause a decrease of vitality [AD58, AD61, AD65, AD69]. In most cases, stressors do not act individually, but several at the same time, whereby the interactions can be synergic, antagonistic, or overlapping. This, and the different ways in which individual plant species react to different stressors make it difficult to assign plant symptoms to specific stressors [AD61, AD73].

To detect vitality disturbances with remote sensing sensors, the stress symptoms must result in a sufficiently large change in reflection for a sensor to measure them. Typical symptoms of deteriorated forest health causing a change in spectral reflectance are changes in pigment and foliage structure up to complete discoloration, defoliation or even dieback [AD65, AD68]. In a stressed leaf, the chlorophyll content decreases and the remaining pigments, such as xanthophyll and carotene, cause a yellow-red discolouration and a flattening of the spectral curve [AD66]. Significant reflectance changes can also be caused by burnt material, bare ground or a vertical or horizontal restructuring of the vegetation because of the disturbance [AD68].

The detectability of vitality disturbances depends on the spectral, spatial and temporal characteristics of the disturbance and the object of interest (from single tree level up to forest level). Since disturbances represent a decrease in vitality, the same spectral ranges described in 5.1.1 are suitable for detecting these symptoms. To fit the spatial dimensions of the disturbances under investigation, the spatial resolution of the selected data basis is crucial. Considering the temporal dynamics of disturbances substantial challenges arise for their detection [AD68]. In forest ecosystems, changes can be divided into three classes: seasonal changes that affect plant phenology caused by temperature and rainfall interactions, gradual changes that follow a trend caused for example by climate variability or land management, and abrupt changes caused by disturbances [AD74]. Depending on the type of stressor, the vitality decrease may occur immediately or over a period of years. Compared to abrupt disturbances such as forest fires, slow-acting stressors such as drought are more difficult to detect. Thus, depending on the stressor process, a suited time scale and data basis are fundamental for successful detection. Since the occurrence of abrupt disturbances is often followed by a rapid recovery of surviving or growing colonising plants, a sufficiently high temporal resolution is important for successful disturbance detection. The sensor choice plays a central role considering all these aspects [AD68].

From a technical perspective, disturbances are changes in vitality which can be identified by analysing differences between two or multiple remote sensing acquisitions taken at different times. These changes can be measured in terms of frequency, intensity, their spatial and temporal extent, stability, and rates. Bi-temporal methods, which compare two images, are the change detection methods with the longest application history and often only distinguish between changed and unchanged features. For example, the widely used and robust change vector analysis (CVA) derives additional information about the change, such as the change intensity and direction of the spectral behaviour.

For long-term monitoring of forest development, many studies use multi-temporal data sets, which have a low temporal resolution of one observation or less per year. This change analysis methodology is called trajectory analysis and is suitable for studying long-term trends, but not seasonal patterns and disturbances.

Since both time scales are not suitable to detect short- and long-term disturbances, long-term time series with a high temporal resolution are the best option. Table 3 compares the three change detection approaches in more detail with each other. In remote sensing, time series are data sets consisting of a

series of images taken of the same area at different times [AD75]. To detect disturbances, often VI time series are used to detect deviations from phenology and vitality changes. With the increasing availability of high-resolution, multi-spectral sensors with high temporal resolution like Sentinel, Terra, Landsat, and RapidEye, VI time series have become a widely used tool for analysing forest vitality dynamics [AD76, AD77]. The choice of a suitable VI is crucial, especially for global applications. Two widely used spectral indices for condition monitoring are the NDVI and the EVI, described in 5.1.1 [AD75. AD76]. Depending on the temporal resolution of the platform and the local cloud cover, the observation frequency can vary greatly. This can result in irregular VI time series with large gaps after, for example cloudy pixels have been filtered to remove outliers and noise. As many time series analysis methods are only applicable to regular time series, missing values are often interpolated in the pre-processing, which can lead to poor performance and undesirable bias in the results [AD75. AD76].

A suitable time series analysis method must therefore be able to deal with irregular time series and to filter out disturbances from phenology and trends. A widely used and established method for time series analysis in remote sensing that meets these requirements is the "Breaks For Additive Seasonal and Trend" (BFAST) method. It decomposes a time series into its seasonal, trend and remainder components and detects breakpoints as abrupt changes by using statistical change detection methods. With BFAST, disturbances can be characterized by their magnitude, date and direction, with the need to select a threshold for statistical significance, but without the need for selecting a reference period or change trajectory. This, and the fact that it can be flexibly applied to different data types and sensors, makes BFAST suitable for monitoring and alarm systems. By now, the method has been successfully applied to VI time series in forest ecosystems in numerous studies and, according to Verbesselt et al. (2010), is able to detect changes of > 0.1 NDVI with seasonal amplitudes of up to 0.5 NDVI [AD74].

Next to the BFAST method other time series methods exist:

- Chávez (2022) npphen R library: no terra support, raster based, worse than bfast [AD78]
- Simoes (2021) sits R library: not suited for our worflow, worse than bfast [AD79]
- Ghaderpour (2020) JUST python library [AD76]

Table 3: Comparison of change detection approaches [AD75]

	Bi-temporal analysis	Trajectory analysis	Time series analysis
Date of change	Sometime between both recording times	Rough estimation, not exact	With good temporal precision, depending on the time series density
Advantages	small data volume; many algorithms; computationally efficient	moderate data volume; good balance of outcome and effort; trends and abrupt changes detectable	detailed understanding of temporal dynamics, seasonal effects, inter- & intra-annual dynamics detectable; all observations used; no scene selection or compositing required; almost gapless process characterization; option of time series decomposition

	Bi-temporal analysis	Trajectory analysis	Time series analysis
Disadvantages	processes and their spatio-temporal characteristics are not detectable; thresholding required to separate change from no-change	data selection and/or compositing required; areas of frequent cloud coverage; seasonal variation & dynamics are not detectable; data availability in some regions	big data volume; comprehensive preprocessing requires automation; data availability in some regions, computationally very inefficient
Methods	CVA, Post Classification Comparison, sustained change	LandTrendr	BFAST, BFAST Lite, fastCPD

Scientific Trade-Off Analysis

Based on the previous analysis and preliminary results, we compare the advantages and disadvantages of the following three methods: sustained change, BFAST Lite, and fastCPD.

Sustained change is a bi-temporal analysis method. Its advantages are that it requires only two images to compare and detect changes. However, this method is extended to incorporate more time steps with minimal additional computational complexity. For two images at times n and $n-1$, t_n and t_{n-1} respectively, the percentage change, $\Delta Yperc$, is defined at each pixel by the equation

$$\Delta Y_{perc,n} = (t_n - t_{n-1})/t_{n-1} * 100$$

The above procedure is computed for all time-steps. The result would be a vector of percentage changes, i.e., $\Delta Y_{perc,i}$ where $i = 1, \dots, n$ represents all time-steps. From this vector, the sustained change metric, $Y_{sustained}$, is calculated by

$$Y_{sustained} = \Delta Y_{perc} \cdot I(\Delta Y_{perc,i,i+1,i+2} > thr)$$

Where $I(X > thr)$ is an indicator function which is 1 when the condition is fulfilled, and 0 otherwise. The condition in this case is whether or not there is more than a specified threshold, thr, of change at the current time step and the following two time steps. For the Case study of Germany, the chosen threshold was 30%.

Because the method can function with any length of image time-series, the amount of data needed is minimal. Computationally it does not take long to calculate. This makes it particularly scalable and transferable to other areas of interest. Particularly, it would perform fast on very large areas of interest. It can still provide a magnitude and direction of change. Particularly, the proposed sustained change metric can work with more than two images, in which case it can also provide information about the spatial and temporal dynamics of the changes being detected. One of the main disadvantages is that a threshold needs to be chosen. This is not different than other methods. In the sustained change methodology, the threshold chosen is in terms of percentage change within two consecutive images. If there are only two images compared, then no information about the spatio-temporal characteristics of disturbances can be inferred.

The BFAST method is a time-series analysis method. Its main advantage is that it can use all available data, and gaps are allowed in this context. The BFAST decomposes the time-series iteratively into a piecewise linear trend and a seasonal model, with the equation

$$Y_t = T_t + S_t + e_t,$$
$$t = 1, \dots, n$$

Where Y_t is the observed data at time t, T_t is the trend component, S_t is the seasonal component, and e_t is the remainder component. The model assumes T_t is a piecewise linear model with m breakpoints at times $t_1^*, \dots, t_m^*$, and thus:

$$T_t = \alpha_j + \beta_j t$$
$$t_{j-1}^* < t \leq t_j^*$$
$$j = 1, \dots, m$$

Where α is the intercept of the linear model, and β is the slope of the linear model. The seasonal component is calculated by:

$$S_t = \sum_{i=1}^{s-1} \gamma_{i,j}(d_{t,i} - d_{t,0})$$

Where $d_{t,1}$ is a dummy variable, equal to 1 if t is in season i and 0 otherwise.

To determine if a break is present in a time-series, the Moving SUM (MOSUM) test is implemented. This test is based on the residuals of an ordinary least squares (OLS) regression. If the test indicates a statistically significant change ($p - value < 0.05$), break points are calculated iteratively following the steps in [AD80].

The method can also give information about the spatio-temporal dynamics of disturbances. A main disadvantage of the method is that it still takes considerable time to run. The BFAST Lite is a faster breakpoint detection method, developed to improve the computational efficiency of BFSAT – it is several orders of magnitude faster to compute. For the case study of Hessen, the algorithm took 15 hours to run (BFAST: 6 days). Without massive parallel implementation, this method is therefore not able to scale up or transfer to larger areas of interest. A trade-off for running faster is that BFAST Lite does not decompose the time-series into seasonal and trend components. Therefore, it cannot give a detailed understanding of the temporal dynamics, seasonal effects, and inter/intra -annual dynamics. Another disadvantage is that it requires longer time series to be able to detect the seasonality, and a minimum of 4 to 5 years of data are recommended.

The fastCPD method is another time-series analysis methods. The method was chosen because it is a recent development with the express intention to reduce computing time of commonly used change detection methods. One of its advantages is that it computes the changes faster than BFAST Lite, with the area of interest in Hessen taking only 45 minutes to complete. It can also use all of the observations, even in the presence of missing data. Still, the computing time can still be a prohibiting factor when scaling the method up to much larger areas of interest. Another disadvantage is that it requires a time-series model specification, and the optimal model is also location dependent.

5.2 Proof of Concept

5.2.1 Methods selection

5.2.1.1 Vitality

Since VI are well-researched, have shown robustness and are comparably simple in use, a NDVI based method for tracking differences in forest area vitality between two points in time was established. It is a pixel-based approach showing forest condition and providing insight in vitality trends for all forest types.

The Approach uses all Sentinel-2 data between 2017 and 2023, which were aggregated monthly and yearly via a best-pixel approach to gather mostly cloud free composites. To identify changes in forest vitality, the NDVI was calculated for each monthly composite, on which basis yearly NDVI maximum values were calculated in the next step. These maximum NDVI composites were then compared between years to identify forest disturbances and timber harvesting as well as forest areas without change or areas with regrowth. A time-series analysis of the monthly maximum NDVI composites reflects the NDVI-based vitality trend that shows vitality gain and loss (Figure 7).

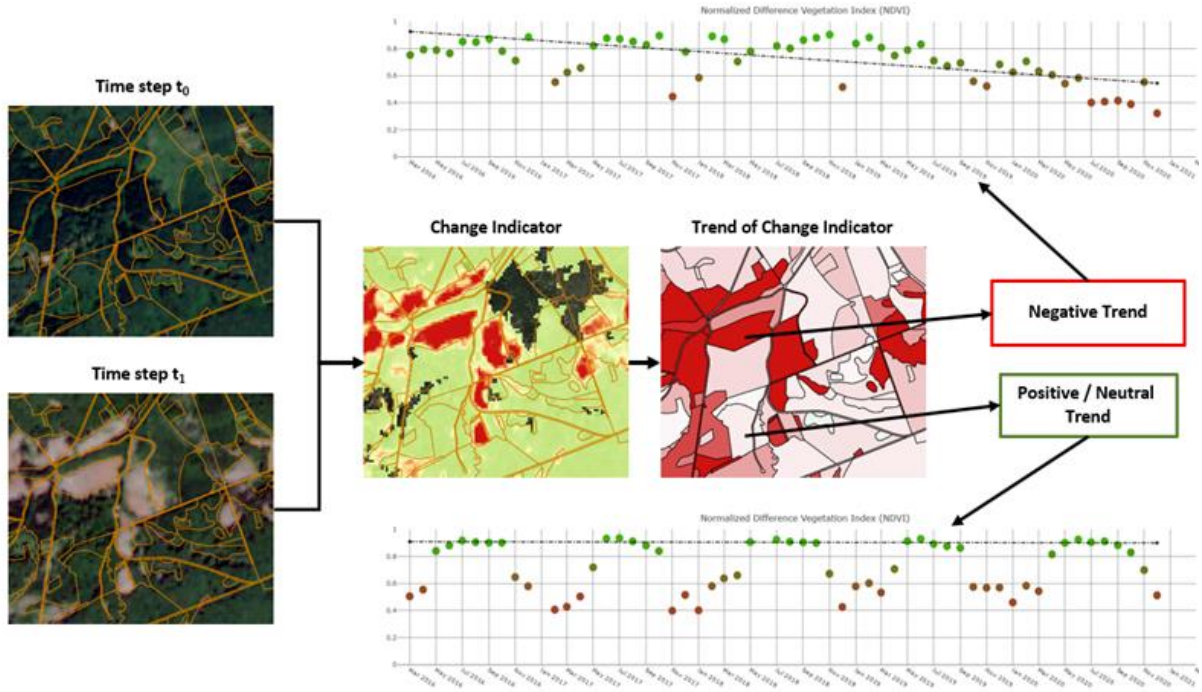

Figure 7. Visualisation vitality approach

5.2.1.2 Disturbance

Based on the vitality testing the EVI is chosen to detect forest disturbances. The methods tested in this analysis are common breakpoint or change detection algorithms available in open-source software. The satellite time-series data used for the analysis is derived from freely available data repositories. The methods were chosen to represent a variety of approaches that are complementary and state-of-the-art. The methods chosen for comparison are the sustained change metric, the BFAST Lite algorithm, and the fastCPD method. These methods are all available within R packages.

When considering which method to use, it is important to consider the scalability and transferability of each method. The methods chosen operate on pixel time-series, and so their implementation can be easily transferred to other areas of interest. However, the question of scalability relates also to their

computational run time. In the tested area of Hessen, the results indicate that the BFAST Lite and fast CPD methods are not scalable to larger areas of interest. The sustained change method is scalable to larger areas of interest and thus recommended for such cases. For the case of smaller areas of interest, the BFAST and BFAST Lite methods remain a viable option.

Then test different BFAST Workflows and parameter settings (different models).

5.2.2 Synthesis

5.2.2.1 Vitality

The chosen methodology was particularly convincing due to its simple applicability to large-scale data sets. By determining the NDVI values for two selected time periods, it has already been possible to obtain results for all forest areas in Ethiopia. This method can be used to analyse the vitality status of forest areas at a specific point in time as well as over a period of time.

However, for a precise application to specific study areas such as forests, a land classification is required. Only in this way can NDVI values of forest areas be specifically distinguished from other dense vegetation areas.

5.2.2.2 Disturbance

The case study focused on forest area within the state of Hessen in Germany. All the methods were tested on the same data and compared according to the information they can provide regarding the disturbance, and their time of implementation.

The presented methods give an insight into various characteristics of forest disturbances. The timing of the event is captured, its spatial extent, temporal duration, as well as the magnitude of disturbance can be analysed. It is important to note that these characteristics are affected by the temporal and spatial resolution of the data. Nevertheless, this methodology allows for an automated analysis of forest disturbances that can be carried out in any area of interest around the globe.

We choose the change threshold of 30% to showcase the method. The threshold of 20% shows similar spatial patterns, while higher thresholds fail to capture coherent spatial patterns. This can hint at a high false negative rate, as then it becomes unable to detect any change.

The results for the sustained change method are shown in Figure 8. The maps show both the timing and the magnitude of the change. We observe large areas of sustained change throughout the analysed years. The calculation of disturbances took less than 10 seconds to run.

The method is capable of detecting more than one disturbance in a single pixel. The map shows only the largest disturbance per pixel. This also highlights areas with consistently large magnitudes, e.g., the northwest region appears to have experienced widespread change in the years 2010/2011.

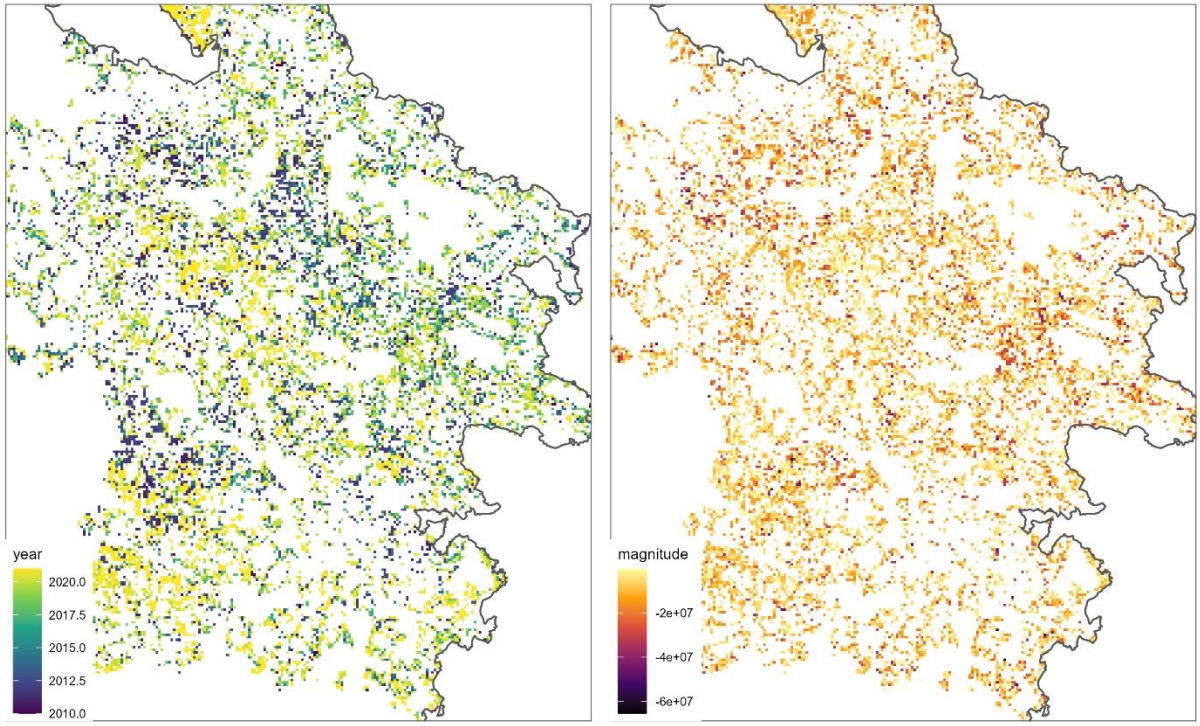

Figure 8. Sustained change results for Hessen, with a threshold of 30% change.

5.3 Final Specification of EO solution

5.3.1 Vitality

The final vitality product is based on a comparison of two Sentinel 2 time series of any study area. Therefore, the spatial resolution of the output raster file is bound to the 10m resolution of the Sentinel 2 product.

The time series can be freely selected by the user, as can the desired study area. The input format for the desired study area can be any vector file, e.g. a Shapefile or Geojson.

The calculation of the maximum NDVI is based on the formula:

$$NDVI = \frac{NIR - RED}{NIR + RED}$$

The time change is calculated subtraction between the to time steps.

The output raster is an 10m resolution NDVI normalized raster file, showing the vitality change between chosen time steps (Figure 9).

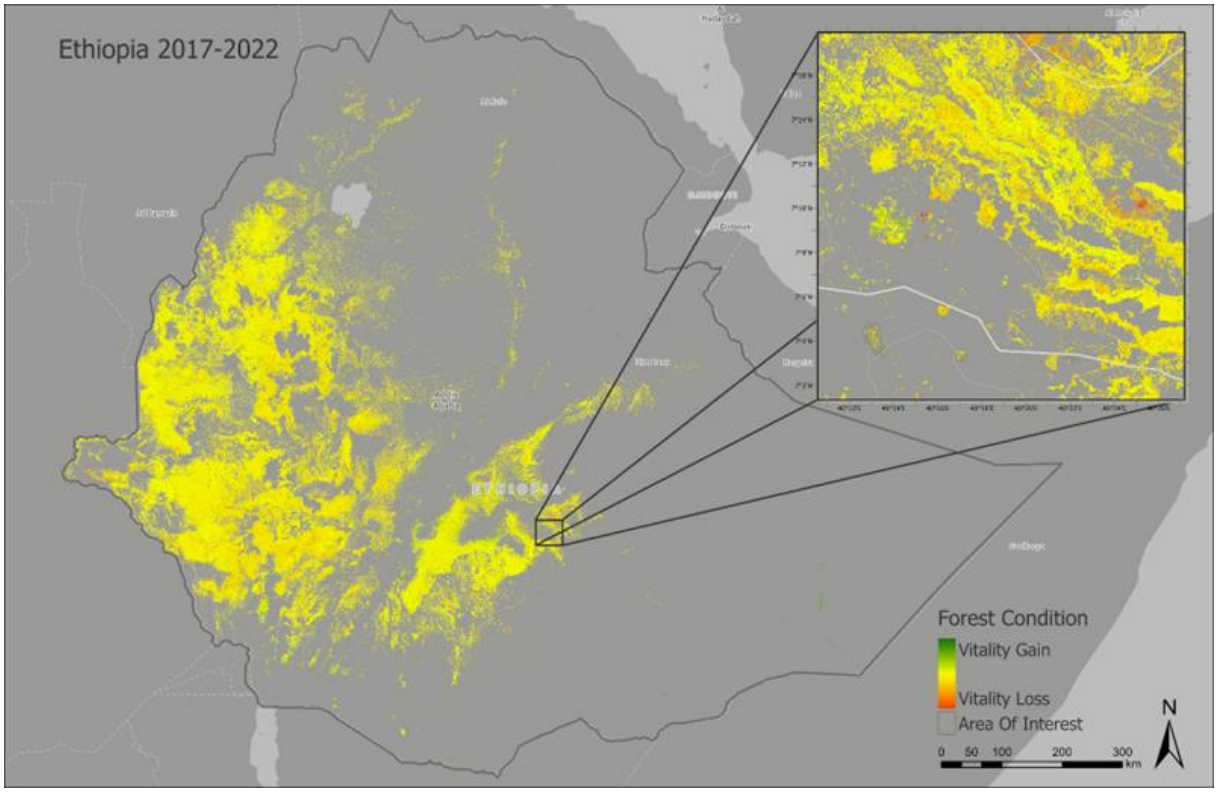

Figure 9. Visualisation of the final EO-vitality product

5.3.2 Disturbance

Disturbances are an integral part in forest ecosystems, influencing their stand, structure, and regeneration. Although there is no single definition for a disturbance that satisfies all scientific and societal questions, it can be described as a negative deviation from the long-term phenology and thus a decrease in vitality.

To detect vitality disturbances with remote sensing sensors, the stress symptoms must result in a sufficiently large change in reflection for a sensor to measure them. Typical symptoms of deteriorated forest health causing a change in spectral reflectance are changes in pigment and foliage structure up to complete discoloration, defoliation or even dieback. Spatial and temporal characteristics of the disturbance and the object of interest (from single tree level up to forest level) also influence greatly the detectability of vitality disturbances by sensors.

From the methods tested and analysed in this section, we chose the sustained change method to measure vitality disturbance in the national demonstrator. It is a bi-temporal analysis method which requires only two images to compare and detect changes, an optional forest mask and the definition of an area of interest (Table 4). However, this method is extended to incorporate more time steps with minimal additional computational complexity. For two images at times n and $n-1$, t_n and t_{n-1} respectively, the percentage change, $\Delta Yperc$, is defined at each pixel by the equation:

$$\Delta Y_{perc,n} = (t_n - t_{n-1})/t_{n-1} * 100$$

Table 4. Input datasets for sustained change calculation

Dataset	Use	Characteristics
Sentinel 2 Data	Atmospherically corrected surface reflectances in cartographic geometry.	Coverage: Gobal Resolution: 10 m Multispectral files (time span specified during data input in workflow)
Copernicus Global Land Service	Classification of land cover out of which the forest classes for the entire world can be extracted	Single layer, GeoTIFF files. CRS: EPSG 4326 Resolution: 100 m Version: 3.0 Product years: 2015-2019 Twelve forest classes
Global Administrative Areas (GADM)	Helpful in the standard delineation of landscapes across different regions	Shapefile/Geopackage Version: 4.1 Up to four administrative levels

Although the spatial extent, the temporal duration and the magnitude of the disturbance largely depend on the spatial and temporal resolution of the data, the selected methodology allows for an automated analysis of forest disturbances that can be carried out in any area of interest around the globe.

The results for the sustained change method showed large areas of sustained change throughout the analysed years. Computationally it does not take long to calculate (the calculation of disturbances in the Hessen example took less than 10 seconds to run). These factors make this method particularly scalable and transferable to other areas of interest, with confidence that it would perform fast on very large areas.

6 Change in Erosion Risk / Landslide Risk (FER)

6.1 Theoretical background

As Grimm from the European Soil Bureau (JRC) describes it in a report [AD24], soil erosion is a natural process, occurring over geological time, and most concerns about erosion are related to accelerated erosion, where the natural rate has been significantly increased by human action. These actions have generally been through stripping of natural vegetation for cultivation, indirect changes in land cover through grazing and controlled burning or wildfires, through re-grading of the land surface and/or a change in the intensity of land management, for example through poor maintenance of terrace structures. Increasing use of mechanised cultivation has also led to a substantial increase in rates of tillage erosion.

Erosion literature commonly identifies 'tolerable' rates of soil erosion, but these rates usually exceed the rates, which can be balanced by weathering of new soil from parent materials, and can only be considered acceptable from an economic viewpoint. It is clear that on most productive land there is an overall loss of soil material that is becoming increasingly unacceptable.

The Global Soil Partnership mechanism of the FAO [URL01] reports that soil erosion is one of the ten major soil threats, identified in the Status of the World's Soil Resources Report [AD25]. Soil erosion is defined as the accelerated removal of topsoil from the land surface mainly through water, wind and tillage. It occurs naturally under all climatic conditions and on all continents, but it is significantly increased and accelerated by unsustainable human activities through intensive agriculture, deforestation,

overgrazing and improper land use changes. Soil erosion rates are much higher than soil formation rates, meaning its loss and degradation is not recoverable within a human lifespan.

Soil erosion affects soil health and productivity by removing the highly fertile topsoil and exposing the remaining soil. It decreases agricultural productivity, degrades ecosystem functions, amplifies hydrogeological risk such as landslides or floods, causes significant losses in biodiversity, damage to urban infrastructure and, in severe cases, leads to displacement of human populations. Soil erosion can affect the infiltration, storage and drainage of water in the soil, resulting in waterlogging and water scarcity. Although soil erosion has a direct impact on farmers, it also has effects outside of agriculture. It has implications for our environment and health including on water quality, the energy sector, urban infrastructure, and our landscapes.

Each type of erosion (water, wind and tillage) involves distinct processes that detach and transport soil; hence each also requires different approaches to decrease associated rates of erosion. In some regions of the world all three types of erosion operate simultaneously in the landscape, and the identification of the processes occurring at a location is a key element of erosion control. Other forms of erosion may also be of importance. Poesen (2018) [AD26] includes soil erosion by land levelling and soil quarrying, by crop harvesting, and by explosion cratering and trench digging as other sources of erosion. As well, soil erosion by mass wasting - through slumping, debris flows and other means - is of major importance in particular landscapes.

Water erosion occurs mainly when overland flow transports soil particles detached by drop impact or run-off, often leading to clearly defined channels such as rills or gullies (Figure 10).

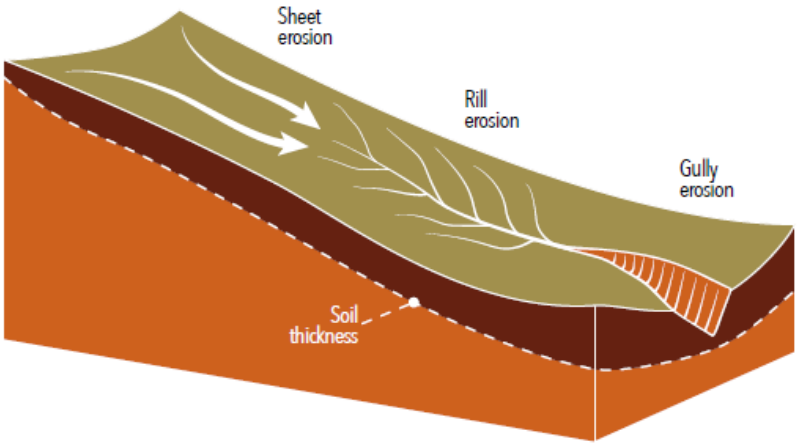

Figure 10. Schematic diagram of the position of sheet, rill, and gully erosion in a simple hillslope system

Wind erosion occurs when dry, loose, bare soil is subjected to strong winds and soil particles are detached from the soil surface and transported elsewhere. Tillage erosion is the direct down-slope movement of soil by tillage implements and results in soil redistribution within a field. But the process that affects the greatest land area is water erosion.

Vegetation has a significant effect on all of the water erosion processes, which can be partly explained because vegetation protects the soil from raindrop impact and retards the formation of surface seals; the former reduces raindrop detachment, and the latter decreases the volume of run-off. With increasing vegetation density and as we move from cropland to grassland to forest, both an increase in resistance by the soil to concentrated flow erosion and a decrease in run-off discharge during a rainfall event are expected [AD27].

Soil erosion can be reduced through the implementation of sustainable management practices such as keeping the soil surface always vegetated. This is particularly valid in agriculture where the use of cover

crops can have a significant impact. It can also be prevented by limiting tillage, or by building terraces. Policy-makers, by integrating these practices into effective policies, can help fostering their implementation on the ground. They can be supported by scientists, who continuously contribute to improve knowledge, and create innovative solutions and technologies to assess, control and prevent soil erosion. By raising awareness or by planting vegetation to protect the soil, in gardens or in scarcely vegetated areas, soil erosion can be extensively reduced.

Scientific Trade-Off Analysis

As explained by Grimm in the European Soil Bureau (JRC) report [AD24], various approaches can be adopted for assessing the soil erosion risk. A distinction can be made between expert-based and model-based methods.

For instance, the soil erosion risk map of Western Europe by De Ploey (1989) [AD28], is an example of an expert-based approach. The resulting map shows the areas where erosion processes are considered to be important by local experts. Nevertheless, a limitation of this approach is that the author does not define clearly the criteria used to delineate the areas deemed to be at risk [AD29].

Factorial scoring is another example of expert-based approach that can be used to assess erosion risk [AD30], based on factorial scores for soil erodibility (4 classes), erosivity (3 classes) and slope angle (4 classes). The scores are multiplied, giving a combined score that represents potential erosion risk. To assess actual soil erosion risk, the potential erosion risk map is combined with a land cover factor (2 classes). This approach has been used for the CORINE programme in 1992 to calculate a soil erosion risk map of the Mediterranean region.

Montier et al. (1998) [AD31] also developed an expert-based method based on scores that are assigned to factors related to land cover (9 classes), the soil's susceptibility to surface crusting (4 classes), slope angle (8 classes) and erodibility (3 classes). The method, used over the whole French territory, takes into account the different types of erosion that occur on cultivated areas, vineyards, mountainous areas, etc., accounting for the interaction between soil, vegetation, slope and climate to some extent.

There are several other examples of expert-based methods developed for soil erosion risk assessment. For instance, the Global Assessment of Soil Degradation (GLASOD) project, whose main objective was to bring to the attention of decision makers the risks resulting from inappropriate land and soil management to the global well-being, allowed identifying areas with a subjectively similar severity of erosion risk, irrespective of the conditions that would produce this erosion.

A fourth example of expert-based approach is the analysis and mapping of soil problem areas (Hot Spots), commissioned by the EEA and conducted using data from the literature on actual sediment losses for a number of locations in Europe. The aim was to emphasize on the need for a pan-European policy on soil, identifying 'hot spots' of degradation in Europe and examining environmental impacts leading to change and particularly degradation of soil function. In this case, expert knowledge is used to identify broad zones for which the erosion processes are broadly similar. However, the spatial representation of areas at risk is too general to be of use to policy makers.

As for the expert-based methods, there is a lot of studies using model-based approaches for soil erosion risk assessment. A wide variety of models are available and can be classified in a number of ways. The subdivision can be done on the time scale for which a model can be used: some models are designed to predict long-term annual soil losses, while others predict single storm losses (event-based). Alternatively, a distinction can be made between lumped models that predict erosion at a single point, and spatially distributed models. Another possible division is the one between empirical and physically-based models.

The Universal Soil Loss Equation (USLE) is an empirical soil model developed by Wischmeier and Smith, (1978) [AD32]. Originally, USLE was developed mainly for soil erosion estimation in croplands or gently

sloping topography. The USLE quantifies soil erosion as the product of six factors representing rainfall and run-off erosivity (R), soil erodibility (K), slope length (L), slope steepness (S), cover and management practices (C), and supporting conservation practices (P) [AD33]. This empirical equation is based on the statistical analysis of more than 10,000 plot-years of data of sheet and rill erosion on plots and small watersheds [AD34].

The Revised Universal Soil Loss Equation (RUSLE) [AD35] has been developed to more accurately estimate soil loss from both crop and rangeland areas, maintaining the basic structure of the USLE model but incorporating the results of additional research and experience obtained since the 1978 publication of USLE by Wischmeier and Smith. Originally, these models were designed to estimate long-term annual erosion rates on agricultural fields.

Morgan et al. (1984) [AD36] presented a semi-empirical model for predicting annual soil loss from field-sized areas on hillslopes. The Morgan–Morgan–Finney (MMF) model used the concepts proposed by Meyer and Wischmeier (1969) [AD37] to provide a stronger physical base than the Universal Soil Loss Equation [AD32], yet retain the advantages of an empirical approach regarding ease of understanding and availability of data. The model was validated by the authors using erosion plot data for 67 sites in 12 countries and then applied to simulate erosion over a 100-year period in Malaysia under shifting cultivation.

The MMF model separates the soil erosion process into two phases: the water phase and the sediment phase. The water phase determines the energy of the rainfall available to detach soil particles from the soil mass and the volume of run-off. In the erosion phase, rates of soil particle detachment by rainfall and run-off are determined along with the transporting capacity of run-off.

A revised version of the MMF model has been proposed by Morgan (2001) [AD38], taking account the need to improve the description of the processes of erosion and the requirement of users for better guidance on the choice of input parameter values. Changes have been made to the way soil particle detachment by raindrop impact is simulated, accounting for plant canopy height and leaf drainage, and a component has been added for soil particle detachment by flow.

The Agriculture Research Service of the United States Department of Agriculture (USDA-ARS) initiated the Water Erosion Prediction Project (WEPP) in 1989 in response to customers' needs, followed by a decade of development and testing [AD39]. The simplest WEPP model simulation is for a single storm event and a single hillslope profile, where empirical equations are used to predict channel transmission losses and peak run-off rates. The WEPP model is a process-based, continuous, distributed parameter, hydrology, soil erosion prediction and sediment delivery system. Ascough et al. (1997) [AD40] reported that the WEPP model should not be used for watersheds larger than 40 ha and hillslope lengths exceeding 100 m.

In Europe, the Pan-European Soil Erosion Risk Assessment project [AD41] proposes a physically based and spatially distributed model combining the effect of topography, climate and soil into a single integrated forecast of run-off and soil erosion on a 1 sq. km grid. The model addresses run-off more directly than other process-oriented models.

6.2 Proof of Concept

6.2.1 Synthesis

The literature review shows that the soil erosion risk assessment topic has been and is still largely studied. Despite the important number of expert-based approaches developed in the various studies and covering different areas of interest, a recurring problem with most methods based on scoring is that the results are affected by the way the scores are defined. In addition to this, classifying the source data results in information loss, and the results of the analyses may depend strongly on the class limits and the number of classes used. Moreover, unless some kind of weighting is used each factor is given equal weight, which is not realistic. If one decides to use some weighting, choosing realistic values for the weights may be difficult. The way in which the various factors are combined into classes that are functional with respect to erosion risk (addition, multiplication) may pose problems also (Morgan, 1995) [RD19]. Finally, as factorial scoring produces qualitative erosion classes, the interpretation of these classes can be difficult. Therefore expert-based methods are not adapted in the context of SDG forest-related indicators.

On the contrary, the availability of digital datasets in recent years has facilitated application of the model-based approach. Generally, the choice for a particular model largely depends on the purpose for which it is intended and the available data, time and money. Ideally, the model performances should be even whatever the location (transferability), and the data requested in input should not be too difficult to collect. Therefore, the model selection is guided by the following criteria:

- The model must be adapted to assess the soil erosion risk at a global scale.
- The datasets needed to feed the model have to be available globally.
- To satisfy the previous criterion, the number of input datasets has to be reduced (as much as possible).
- The model must be as simple as possible.

Although the MMF model has proved simple to use and is able to give reasonable estimates of annual run-off and erosion, some input parameters are difficult to determine. In particular, the topsoil rooting depth gives problems of definition since it describes the effective hydrological depth within which the storage of water affects the generation of run-off.

Regarding the WEPP model, Chandramohan et al. (2015) [AD42] noted that its major advantage over empirical models is that being a physically-based model, it takes into account processes/events that influence erosion. However, the model under-predicted soil loss because of the large data requirement and many number of model parameters related to soil and crop management which is impractical to collect or measure in studies of large scale.

In the end, the RUSLE model seems to best fit to the specifications, in particular because according to (Grimm et. al., 2002) [AD24]:

- It is one of the least data demanding erosion models that has been developed and applied widely at different scales.
- It is widely used because of its relative simplicity and robustness [AD43].
- It has a standardized approach.

After this state-of-the-art review, the RUSLE model has been used and tested over various areas of interest to analyse its performances in different configurations. To achieve that, some test sites have been chosen in several countries (Brazil, Colombia, Cameroon and Ivory Coast) and various datasets have been used in input to determine the influence on the model behaviour.

The complete description of all this experimental phase (test sites, input datasets, algorithm implementation, results evaluation) is reported in the Proof of Concept (PoC) document. The analysis of all the tests conducted proves that the RUSLE model performances are satisfying. Therefore, it seems adapted in the context of this project.

6.3 Final Specification of EO solution

In theory, the mathematical implementation of the RUSLE model is based on the following equation:

$$A = R \times K \times LS \times C \times P$$

Where:

- A is the average annual soil loss (in ton ha-1 year-1);
- R is the rainfall erosivity factor (in MJ mm ha-1 h-1 year-1);
- K is the soil erodibility factor (in ton ha h ha-1 MJ-1 mm-1);
- LS is the slope length and steepness factor (dimensionless);
- C is the cover management factor (dimensionless);
- P is the conservation or support practices factor (dimensionless).

Nevertheless, considering the very poor availability of P factor datasets (even more at the global scale), the final implementation of the equation only relies on the first four input parameters (R, K, LS and C), choosing to discard the P factor.

For listing the datasets needed in input, a distinction has to be made between the layers available only at the European scale, or globally. This point is important because the global layers generally offer poorer spatial resolution than those covering only the European territory. Therefore, European datasets must be preferred when working over this continent.

Table 5 provides an inventory of all the input datasets that can be used for this EO solution. It is worth mentioning that considering the results of experimental phase and the relatively limited added value brought by the SRTM layer, it has been decided not to keep it among the list of the input layers proposed to the user.

Table 5. Input datasets inventory for the FER / Erosion Risk EO solution

Dataset	Use	Characteristics
Rainfall erosivity dataset in Europe	Direct use as input parameter (R factor)	Coverage: Europe Source: JRC/ESDAC Spatial resolution: 500m Publication: 2015
Global rainfall erosivity dataset	Direct use as input parameter (R factor)	Coverage: Global Source: JRC/ESDAC

Dataset	Use	Characteristics
		Spatial resolution: 30 arc-seconds, ~1km at the equator Publication: 2017
Soil erodibility dataset in Europe	Direct use as input parameter (K factor)	Coverage: Europe Source: JRC/ESDAC Spatial resolution: 500m Publication: 2014
Global soil erodibility dataset	Direct use as input parameter (K factor)	Coverage: Global Source: JRC/ESDAC Spatial resolution: 1km Publication: 2023
Harmonized World Soil Database v2.0	Used to compute the K factor	Coverage: Global Source: FAO Spatial resolution: 30 arc-seconds, ~1km at the equator Publication: 2023
European Digital Elevation Model (EU-DEM)	Used to compute the LS factor	Coverage: Europe Source: EEA Spatial resolution: 1 arc-second, ~30m Publication: 2016
Copernicus DEM - Global Digital Elevation Model (COP-DEM)	Used to compute the LS factor	Coverage: Global Source: EU Copernicus / ESA Spatial resolution: 1 arc-second, ~30m Publication: 2019
CORINE Land Cover	Used to compute the C factor	Coverage: Europe Source: EU Copernicus Land Monitoring Service Spatial resolution: 100m Publication: 2018
Copernicus Global Land Cover	Used to compute the C factor	Coverage: Global Source: EU Copernicus Land Monitoring Service Spatial resolution: 100m Publication: 2019
WorldCover	Used to compute the C factor	Coverage: Global Source: ESA Spatial resolution: 10m Publication: 2021

For the rainfall erosivity and the soil erodibility parameters, the selection between the European or the global datasets will be controlled by a parameter indicating whether the area of interest is located in Europe or not, and filled by the user. For the others input parameters (DEM, LULC), the user will have the

possibility to choose the layers he wants to work with. Of course, the choice must be coherent with the area of interest location. For example, if the user wants to use the EU-DEM or the CORINE Land Cover outside Europe, the model will not be able to execute properly and will eventually crash. In addition, the user also has to provide an area of interest and an optical satellite image.

Once all the input fields are completed, the user can launch the tool to compute the RUSLE model. First of all, the R and K factors are automatically derived and extracted from the appropriate input layer, based on the location value selected by the user. The LS factor can be directly calculated from the DEM layer, whereas it is a little bit more complex for the C factor. Indeed, the satellite imagery is used to compute the FCover which in turn is needed, in addition to the LULC, to calculate the C factor.

When all the factors are ready, the RUSLE equation can be calculated to obtain the soil erosion susceptibility values (in ton/ha/year). Once this average annual soil loss is available, it is then possible to obtain a soil erosion risk classification by applying some predefined thresholds, so that the final soil erosion risk can be assessed (ranging from very low/tolerable to severe). A final step consisting in intersecting the output layers (mean annual soil loss and soil erosion risk classification) with the area of interest is achieved to correspond to the user request.

7 Landscape Metrics (FLM)

7.1 Theoretical background

Growing concerns over the loss of biodiversity have spurred land managers to seek better ways of managing landscapes at a variety of spatial and temporal scales. The developing field of landscape ecology has provided a strong conceptual and theoretical basis for understanding landscape structure, function, and change [AD11, AD12, AD13]. Growing evidence that habitat fragmentation is detrimental to many species and may contribute substantially to the loss of regional and global biodiversity [AD14, AD15] has provided empirical justification for the need to manage entire landscapes, not just the components. The development of GIS (geographical information systems) technology has made a variety of analytical tools available for analysing and managing landscapes. In response to this growing theoretical and empirical support and to technical capabilities, public land management agencies have recognized the need to manage natural resources at the landscape scale. A good example of these changes is in wildlife science. Wildlife ecologists often have assumed that the most important ecological processes affecting wildlife populations and communities operate at local spatial scales [AD16]. Vertebrate species richness and abundance, for example, often are considered functions of variation in local resource availability, vegetation composition and structure, and the size of the habitat patch [AD17]. Correspondingly, most wildlife research and management activities have focused on the within-patch scale, typically small plots or forest stands. However, there has been increasing awareness of the potential importance of coarse-scale habitat patterns to wildlife populations and a corresponding surge in landscape ecological investigations that examine vertebrate distributions and population dynamics over broad spatial scales and including a landscape perspective in policies and guidelines for managing public lands.

Landscape ecology embodies a way of thinking that many see as very useful for organizing land management approaches. Specifically, landscape ecology focuses on three characteristics of the landscape:

1. Structure, the spatial relationships among the distinctive ecosystems or “elements” present—more specifically, the distribution of energy, materials, and species in relation to the sizes, shapes, numbers, kinds, and configurations of the ecosystems.

2. Function, the interactions among the spatial elements, that is, the flows of energy, materials, and species among the component ecosystems.

3. Change, the alteration in the structure and function of the ecological mosaic over time.

Thus, landscape ecology involves the study of landscape patterns, the interactions among patches within a landscape mosaic, and how these patterns and interactions change over time. In addition, landscape ecology involves applying these principles to formulate and solve real-world problems. Landscape ecology considers the development and dynamics of spatial heterogeneity and its effects on ecological processes and the management of spatial heterogeneity [AD18]

The disparity in definition of landscape makes it difficult to communicate clearly and even more difficult to establish consistent management policies. Definitions invariably include an area of land containing a mosaic of patches or landscape elements. Forman and Godron [AD11] define landscape as a "heterogeneous land area composed of a cluster of interacting ecosystems that is repeated in similar form throughout." The concept differs from the traditional ecosystem concept in focusing on groups of ecosystems and the interactions among them. There are many variants of the definition depending on the research or management context. From a wildlife perspective, for example, landscape might be defined as an area of land containing a mosaic of habitat patches, within which a particular "focal" or "target" habitat patch often is embedded [AD16]. Because habitat patches can be defined only relative to a particular organism's perception of the environment (that is, each organism defines habitat patches differently and at different scales), landscape size would differ among organisms [AD19]. However, landscapes generally occupy some spatial scale intermediate between an organism's normal home range and its regional distribution. In other words, because each organism scales the environment differently (for example, a salamander and a hawk view their environment on different scales), there is no absolute size for a landscape; from an organism-centered perspective, the size of a landscape differs depending on what constitutes a mosaic of habitat or resource patches meaningful to that organism.

Patch—Landscapes are composed of a mosaic of patches [AD13]. Landscape ecologists have used several terms to refer to the basic elements or units that make up a landscape, including ecotope, biotope, landscape component, landscape element, landscape unit, landscape cell, geotope, facies, habitat, and site [AD11]. We prefer the term "patch"; but any of these terms, when defined, are satisfactory according to the preference of the investigator. Like the landscape, patches comprising the landscape are not self-evident; patches must be defined relative to the given situation. From a timber management perspective, for example, a patch may correspond to the forest stand; however, the stand may not function as a patch from a particular organism's perspective. From an ecological perspective, patches represent relatively discrete areas (spatial domain) or periods (temporal domain) of relatively homogeneous environmental conditions, where the patch boundaries are distinguished by discontinuities in environmental character states from their surroundings of magnitudes that are perceived by or relevant to the organism or ecological phenomenon under consideration [AD19]. From a strictly organism-cantered view, patches may be defined as environmental units between which fitness prospects or, "quality," differ; although, in practice, patches may be more appropriately defined by non-random distribution of activity or resource utilization among environmental units, as recognized in the concept of "grain response" [AD19].

Patches are dynamic and occur on many spatial and temporal scales that, from an organism-centered perspective, differ as a function of each animal's perceptions [AD19]. A patch at any given scale has an internal structure reflecting patchiness at finer scales, and the mosaic containing that patch has a structure determined by patchiness at broader scales [AD20]. Thus, regardless of the basis for defining patches, a landscape does not contain a single patch mosaic but contains a hierarchy of patch mosaics across a range of scales. From an organism-centered perspective, the smallest scale at which an organism perceives and responds to patch structure is its "grain" [AD20] This lower threshold of heterogeneity is the level of resolution where the patch size becomes so fine that the individual or species stops responding to it, even though patch structure may exist at a finer resolution [AD21]. The lower limit to grain is set by the physiological and perceptual abilities of the organism and therefore differs among

species. Similarly, "extent" is the coarsest scale of heterogeneity, or upper threshold of heterogeneity, to which an organism responds [AD20, AD21]. At the level of the individual, extent is determined by the lifetime home range of the individual [AD20] and differs among individuals and species. More generally, however, extent differs with the organizational level (individual, population, metapopulation) under consideration; for example, the upper threshold of patchiness for the population would probably greatly exceed that of the individual. From an organism-centred perspective, patches therefore can be defined hierarchically in scales ranging between the grain and extent for the individual, deme, population, or range of each species.

Scientific Trade-Off Analysis

Strengths and Weaknesses:

Patch-level metrics (Table 6):

Strengths: Patch-level metrics offer detailed information about individual patches, making them suitable for studying habitat quality, connectivity, and patch dynamics. They provide insights into patch-specific characteristics and can help identify critical patches for conservation efforts. For example, patch size metrics allow us to identify large core habitat areas that are essential for supporting viable populations of species. Shape metrics enable us to assess the complexity and irregularity of patch shapes, which can be important for understanding habitat suitability or vulnerability. Compactness indices help identify patches that are more likely to retain ecological processes due to their reduced perimeter-to-area ratio.

Weaknesses: However, these metrics may not capture the overall landscape pattern or interactions between patches, limiting their ability to assess landscape-level processes and dynamics. While patch-level metrics provide valuable information about individual patches, they do not account for the arrangement or spatial relationships between patches. This limitation can hinder the understanding of landscape connectivity and the movement of organisms across the landscape. Additionally, focusing solely on patch-level metrics may overlook larger-scale landscape processes that operate at the landscape or regional scale.

Class-level metrics (Table 6):

Strengths: Class-level metrics provide valuable insights into the composition and distribution of different land cover classes within the landscape. They allow for the assessment of landscape heterogeneity, aiding in identifying dominant land cover types and their spatial distribution. Class area metrics help identify the abundance and dominance of different land cover classes, providing information about the relative importance of each class within the landscape. Edge metrics offer insights into the spatial configuration and intermixing of different land cover classes, indicating areas of high ecological transition or interface. Shape metrics at the class level help assess the complexity and aggregation patterns of individual land cover classes, which can have implications for habitat suitability or ecological processes. Concretely, Li et al. [AD22], concluded that total number of patches, mean patch size, total edge density, and aggregation index can reflect different patterns successfully at both landscape level and class level.

Weaknesses: However, these metrics do not account for patch shape or configuration, which may limit their ability to capture fine-scale patterns and specific patch interactions. While class-level metrics provide valuable information about the composition and distribution of land cover classes, they do not explicitly consider the shape or arrangement of individual patches. This limitation can be problematic when analyzing landscapes with complex patch shapes or investigating the spatial relationships between specific patches. By focusing on class-level metrics alone, the analysis may overlook important patch-specific dynamics and interactions.

Landscape-level metrics (Table 6):

Strengths: Landscape-level metrics provide an integrated view of the landscape, capturing spatial patterns, fragmentation, and diversity. They offer a holistic understanding of the landscape structure and dynamics, facilitating assessments of ecological processes and landscape-level conservation planning. Fragmentation metrics enable the identification of areas with high levels of patchiness or fragmentation, providing insights into landscape connectivity and potential barriers to species movement. Diversity metrics help assess the variety and evenness of land cover classes, highlighting areas of high ecological heterogeneity or biodiversity. Contagion metrics quantify the spatial arrangement and configuration of different land cover classes, aiding in understanding landscape connectivity and the potential spread of disturbances.

Weaknesses: Nevertheless, these metrics lack detailed information about individual patches, potentially limiting the analysis of specific patch dynamics and interactions. While landscape-level metrics offer a comprehensive understanding of the overall landscape pattern, they may not provide detailed insights into the characteristics of individual patches. This limitation can hinder the assessment of specific patch dynamics, such as patch growth, contraction, or fragmentation. Additionally, landscape-level metrics may not capture fine-scale variations in patch shape or the spatial relationships between specific patches, which are crucial for certain ecological processes or conservation planning efforts. Although it is not exclusively a weakness of landscape-level metrics, it is also important to pay attention to redundance of information from highly correlated indices. For example, Shannon-Weaver diversity, Shannon-Weaver evenness, and dominance are three correlated landscape level metrics and should not be used together [AD22].

Interspersion and Juxtaposition Index (IJI):

Strengths: IJI is a versatile metric compatible with both vector and raster data. It directly measures patch type interspersion, providing valuable insights into the arrangement and adjacency of different patch types. IJI considers the spatial configuration and interspersion of patches, highlighting areas with high levels of patch mixing or intermingling. This metric is particularly useful for analyzing landscapes where patch adjacency plays a crucial role in ecological processes, such as dispersal, species interactions, or ecosystem functioning. By explicitly considering the interspersion of patch types, IJI offers a valuable perspective on the spatial relationships between different land cover classes.

Weaknesses: However, IJI does not explicitly consider the dispersion of focal patch types and is limited to patch edge analysis. While IJI provides insights into the interspersion of patch types, it does not account for the dispersion or spatial extent of specific patch types within the landscape. This limitation can restrict the understanding of how individual patch types are dispersed or distributed across the landscape. Additionally, since IJI primarily focuses on patch edges, it may not fully capture the internal patch characteristics or variations in patch shape or configuration.

Table 6. Landscape metrices (by type and level), their acronyms and units

Scale		Acronym	Metric (units)
Area metrics:			
	Patch	AREA	Area (ha)
	Patch	LSIM	Landscape similarity index (percent)
	Class	CA	Class area (ha)
	Class	%LAND	Percentage of landscape
	Class/landscape	TA	Total landscape area (ha)
	Class/landscape	LPI	Largest patch index (percent)

Scale	Acronym	Metric (units)
Class/landscape	NP	Number of patches
Class/landscape	PD	Patch density (number/100 ha)
Class/landscape	MPS	Mean patch size (ha)
Class/landscape	PSSD	Patch size standard deviation (ha)
Class/landscape	PSCV	Patch size coefficient of variation (percent)
Edge metrics:		
Patch	PERIM	Perimeter (m)
Patch	EDCON	Edge contrast index (percent)
Class/landscape	TE	Total edge (m)
Class/landscape	ED	Edge density (m/ha)
Class/landscape	CWED	Contrast-weighted edge density (m/ha)
Class/landscape	TECI	Total edge contrast index (percent)
Class/landscape	MECI	Mean edge contrast index (percent)
Class/landscape	AWMECI	Area-weighted mean edge contrast index (percent)
Shape metrics:		
Patch	SHAPE	Shape index
Patch	FRACT	Fractal dimension
Class/landscape	LSI	Landscape shape index
Class/landscape	MSI	Mean shape index
Class/landscape	AWMSI	Area-weighted mean shape index
Class/landscape	DLFD	Double log fractal dimension
Class/landscape	MPFD	Mean patch fractal dimension
Class/landscape	AWMPFD	Area-weighted mean patch fractal dimension
Core area metrics:		
Patch	CORE	Core area (ha)
Patch	NCORE	Number of core areas
Patch	CAI	Core area index (percent)
Class	C%LAND	Core area percentage of landscape
Class/landscape	TCA	Total core area (ha)
Class/landscape	NCA	Number of core areas
Class/landscape	CAD	Core area density (number/100 ha)
Class/landscape	MCA1	Mean core area per patch (ha)
Class/landscape	CASD1	Patch core area standard deviation (ha)
Class/landscape	CACV1	Patch core area coefficient of variation (percent)
Class/landscape	MCA2	Mean area per disjunct core (ha)

Scale	Acronym	Metric (units)
Class/landscape	CASD2	Disjunct core area standard deviation (ha)
Class/landscape	CACV2	Disjunct core area coefficient of variation (percent)
Class/landscape	TCAI	Total core area index (percent)
Class/landscape	MCAI	Mean core area index (percent)
Nearest neighbor metrics:		
Patch	NEAR	Nearest neighbor distance (m)
Patch	PROXIM	Proximity index
Class/landscape	MNN	Mean nearest neighbor distance(m)
Class/landscape	NNSD	Nearest neighbor standard deviation(m)
Class/landscape	NNCV	Nearest neighbor coefficient of variation(percent)
Class/landscape	MPI	Mean proximity index
Diversity metrics:		
Landscape	SHDI	Shannon's diversity index
Landscape	SIDI	Simpson's diversity index
Landscape	MSIDI	Modified Simpson's diversity index
Landscape	PR	Patch richness (number)
Landscape	PRD	Patch richness density (number/100ha)
Landscape	RPR	Relative patch richness (percent)
Landscape	SHEI	Shannon's evenness index
Landscape	SIEI	Simpson's evenness index
Landscape	MSIEI	Modified Simpson's evenness index
Class/landscape	IJI	Interspersion and Juxtaposition index(percent)
Landscape	CONTAG	Contagion index (percent)

Trade-Off Analysis (Table 7):

Detail vs. Generalization: Patch-level metrics offer detailed information about individual patches, allowing for a fine-scale analysis of patch characteristics. In contrast, landscape-level metrics provide a more generalized view of the entire landscape pattern, capturing the overall landscape structure and dynamics. The trade-off between detail and generalization lies in balancing the need for specific patch-level information with the broader insights gained from landscape-level metrics.

Fine-scale vs. Landscape-scale: Patch-level metrics focus on the characteristics of individual patches, providing detailed insights into patch-specific processes and dynamics. On the other hand, landscape-level metrics analyze the overall pattern and its ecological implications, allowing for assessments at the landscape or regional scale. The trade-off between fine-scale and landscape-scale analyses involves considering the appropriate scale for the research objectives and the ecological processes of interest.

Complexity vs. Simplicity: Patch-level metrics offer a more detailed and complex assessment of individual patches, capturing their size, shape, and other attributes. In contrast, class-level and landscape-level metrics provide a more simplified perspective by summarizing the characteristics of multiple patches or the entire landscape. The trade-off between complexity and simplicity involves deciding the level of detail required for the analysis and the complexity of the research questions being addressed.

Table 7. Trade off analysis with commonly used landscape metrices

Metric	Strengths	Weaknesses
Patch Density:	Strengths: Patch density provides information about the abundance and distribution of patches within the landscape. It helps identify areas with high fragmentation or patchiness, which can have implications for habitat suitability and species movement.	Weaknesses: Patch density alone does not capture the configuration or interspersion of patches, limiting its ability to assess landscape connectivity or specific patch interactions.
Mean Patch Size	Mean patch size indicates the average size of patches within the landscape. It offers insights into the spatial extent of different land cover classes and can help identify dominant or core habitat areas.	Mean patch size does not consider the shape or distribution of individual patches, potentially overlooking fine-scale patterns and variations in patch configuration.
Edge Density:	Edge density quantifies the amount of edge habitat within the landscape. It provides information about the potential interface between different land cover classes, which is important for species diversity and ecological processes.	Edge density does not distinguish between different types of edges or consider the arrangement or interspersion of patches, limiting its ability to capture specific patch interactions or connectivity.
Landscape Shape Index	The landscape shape index measures the complexity and shape of the landscape boundary. It helps identify irregular or fragmented landscapes and can indicate potential barriers to species movement or dispersal.	The landscape shape index does not provide detailed information about patch-level characteristics or consider the internal configuration of patches.
Shannon's Diversity Index:	Shannon's diversity index assesses the heterogeneity and evenness of land cover classes within the landscape. It provides insights into the biodiversity or ecological diversity of the landscape.	Shannon's diversity index does not explicitly consider the spatial configuration or arrangement of patches, limiting its ability to capture specific landscape patterns or interactions.
Interspersion and Juxtaposition Index (IJI):	Strengths: The IJI measures the interspersion and adjacency of different patch types. It directly quantifies the spatial relationships between patches,	Weaknesses: The IJI does not consider the dispersion or spatial extent of specific patch types, and it is limited to patch edge analysis. It may not capture fine-scale variations in patch shape or the spatial relationships between specific patches.

Metric	Strengths	Weaknesses
	providing valuable insights into patch mixing or intermingling.	

Regardless of the scale of analysis, the use of landscape indices requires understanding of the limitations and correct interpretation of results [AD04]. An important limitation with the hundreds of landscape metrics that are available today is that many of them are correlated to each other, making their interpretation more difficult [AD07, AD08]. Useful metrices should be independent from each other, and many authors choose some sort of correlation algorithm to filter out duplicate information when selecting metrices [AD03, AD07]. The selection methods compared in this document included the popular Pearson correlation (alone) and Pearson correlation with beta ranking, which were carried out such that each metric was minimally correlated with other metrices [AD02, AD03].

Pearson correlation - assumes a linear relationship and that data is normally distributed. It is based on covariance and standard deviations of the original data and is defined by the equation:

$$r_{xy} = \frac{\sum_{i=1}^{n}(x_i - \bar{x})(y_i - \bar{y})}{\sqrt{\sum_{i=1}^{n}(x_i - \bar{x})^2}\sqrt{\sum_{i=1}^{n}(y_i - \bar{y})^2}}$$

It is suitable for the data in our test site because it is continuous and measures the strength and direction of the linear relationship between variables. Its values range between -1 (perfect negative correlation) and 1 (perfect positive correlation), with 0 indicating no linear correlation.

Correlation tests have been extensively used in the literature to select landscape metrices within sustainable forest management [AD02-AD09]. It is often good practice to calculate multiple correlation coefficients to gain a better understanding of the data [AD10]. All correlation tests were run on the patch, class, and landscape levels. However, the number of classes need to be >4 for the correlation algorithms to have any significant results. In our case, with 3 classes per landscape, the decision for landscape metric selection on the class level needs to be performed by expert judgement.

This trade-off analysis emphasizes the importance of considering multiple landscape metrics and their strengths and weaknesses in ecological research and conservation planning. By carefully selecting and integrating relevant metrics, researchers and land managers can gain a comprehensive understanding of landscape patterns, processes, and their implications for biodiversity conservation, ecosystem functioning, and sustainable land use.

7.2 Proof of Concept

7.2.1 Methods selection

The landscape metrics utilized in this analysis were calculated using established indices and commonly used software tools in landscape ecology. The data required for the analysis included spatial data sets representing land cover classes and appropriate boundary delineations. The metrics were derived through rigorous processing steps to ensure the accuracy and reliability of the results. Two widely used methods for metric selection were used here: Pearson correlations and β-score ranking followed by Pearson correlation. The underlying reason for the use of correlation algorithms was the need to filter redundant information from highly correlated landscape indices. Despite the abundance of metrics easily

calculable through libraries like 'landscapemetrics' and the risk of correlation between them, it is important to consider multiple metrics to capture different aspects of landscape patterns comprehensively.

Therefore, when selecting a set of landscape indices for future analysis, the user must consider redundancies and balance the strengths and weaknesses of each index. Moreover, the explored method with the β-score ranking provides an additional layer of complexity, which tests for an index ability to capture changes in landscape pattern [AD03]. In this case, two important criteria for selection are combined in this method, which is easily transferable to any type of landscape. The β-score and Pearson correlation method is thus chosen as comparatively more robust than the Pearson correlation method alone and is suggested for future analyses of new test sites.

7.2.2 Synthesis

7.2.2.1 Germany

Our analysis focused on nine municipalities located in the German Federal State of Hesse: Alheim, Bebra, Cornberg, Nentershausen, Morschen, Spangenberg, Sontra, Rotenburg an der Fulda, and Waldkappel. On the patch level, Alheim was taken as an example landscape. On the landscape level, all landscapes are considered.

Table 8 offers a preliminary set of landscape indices following the β-score and Pearson correlation method. The table provides complementary information which is intended to aid the user in the interpretation of selected metrices.

Table 8. Selected landscape metrices on patch (Alheim) and landscape (all municipalities) based on β score ranking and Pearson correlation values. Class level metrices selection must be performed based on expert knowledge.

Acronym	Level	Type	Description	Measures
Area	Patch	Area and edge	Individual patch area. Basic but important metric to characterise a landscape.	Composition
Core area	Patch	Core area	Area within a patch that is not on the edge. Describes patch area and shape simultaneously. CORE values ≥ 0, increases without limit as the patch area increases and patch shape simplifies.	Composition
Shape	Patch	Shape	It describes the ratio between the actual perimeter of the patch and the square root of patch area (adjusting for a square standard).	Complexity
Circle (related circumscribing circle)	Patch	Shape	Ratio between patch area and the smallest circumscribing circle of the patch. Value comparable among patches with different area.	Compactness
Frac (Fractal dimension index)	Patch	Shape	Based on patch perimeter and patch area. It is standardised, therefore scale independent.	Complexity
Enn (Euclidean nearest neighbour)	Patch	Aggregation	Distance [m] to the nearest neighbouring patch of the same type, based on the shortest edge-to-edge distance.	Isolation

Acronym	Level	Type	Description	Measures
			The metric is a simple way to describe patch isolation	
Prd (patch richness density)	Landscape	Diversity	One of the simplest diversity and composition measures. It is a relative measure that is comparable among landscapes with different total areas.	Composition, Diversity
SHDI (Shannon's diversity index)	Landscape	Diversity	Widely used metric in biodiversity and ecology and takes both the number of classes and the abundance of each class into account	Diversity
SIEI (Simpson's evenness index)	Landscape	Diversity	Ratio between the actual Simpson's diversity index and the theoretical maximum Simpson's diversity index. Equals SIEI = 0 when only one patch is present and approaches SIEI = 1 when the number of class types increases while the proportions are equally distributed	Diversity
MSIEI (modified Simpson's evenness index)	Landscape	Diversity	Range of values are $0 \leq MSIEI < 1$. MSIEI = 0 when only one patch is present and approaches MSIEI = 1 as the proportional distribution of patches becomes more even	Diversity

By combining these landscape indices, researchers can gain a more comprehensive understanding of the landscape pattern, including patch abundance, size, configuration, interspersion, diversity, and edge habitat. It is essential to 1) consider the strengths and weaknesses of each index, 2) assess whether an index is capable of capturing changes in landscape patters through the calculation of the β-score, and 3) filter highly correlated indices to avoid duplication of information. In this way, the user can better understand how landscape metrices complement each other to obtain a more robust assessment of landscape structure and its ecological implications.

7.2.2.2 Vietnam

The chosen AOI in Vietnam is located across the municipalities of Kỳ Anh, Kỳ Anh (Thị xã), Ba Đồn, Bố Trạch, Minh Hóa, Quảng Trạch, Tuyên Hóa, in the provinces of Hà Tĩnh, and Quảng Bình. The selected AOI has 199,854.84 hectares, out of which 74.68% is forest. Contrary to the example of Germany, the forest classification used for Vietnam is taken from the Copernicus Global Land Service. Of the forest land cover in the AOI, closed forest evergreen needle leaf is 0.03%, closed forest evergreen broad leaf is 86.94%, closed forest unknown is 1.96%, open forest evergreen broad leaf is 2.08%, open forest unknown is 9% of the total. The other land cover categories are shrubs, herbaceous vegetation, cultivated and managed vegetation/agriculture, urban/built up, bare/sparse vegetation, permanent water bodies, herbaceous wetland, closed forest evergreen needle leaf, closed forest evergreen broad leaf, closed forest unknown, open forest evergreen broad leaf, open forest unknown, and open sea.

Table 9 offers a preliminary set of landscape indices following the β-score and Pearson correlation method. The table provides complementary information which is intended to aid the user in the interpretation of selected metrices.

Table 9. Preliminary set of selected landscape metrices on patch, class and landscape levels for the Vietnamese AOI. Selection based on β score ranking and Pearson correlation values.

Acronym	Level	Type	Description	Measures
Area	Patch	Area and edge	Individual patch area. Basic but important metric to characterise a landscape.	Composition
Contiguity index (contig)	Patch	Shape	Contig assesses the spatial connectedness (contiguity) of cells in patches. The metric coerces patch values to a value of 1 and the background to NA.	Configuration
Core area index (cai)	Patch	Core area	Area within a patch that is not on the edge. Describes patch area and shape simultaneously. CORE values ≥ 0, increases without limit as the patch area increases and patch shape simplifies.	Composition
Number of core areas (Ncore)	Patch	Core area	A cell is defined as core if the cell has no neighbour with a different value than itself (rook's case). The metric counts the disjunct core areas, whereby a core area is a 'patch within the patch' containing only core cells. It describes patch area and shape simultaneously (more core area when the patch is large, however, the shape must allow disjunct core areas). Thereby, a compact shape (e.g. a square) will contain less disjunct core areas than a more irregular patch.	Composition/ Complexity
Radius of gyration (gyrate)	Patch	Area and edge	The distance from each cell to the patch centroid is based on cell center to centroid distances. The metric characterises both the patch area and compactness.	Compactness
Area	Class	Area and edge	Individual patch area. Basic but important metric to characterise a landscape.	Composition
Cai_mn/cai_sd	Class	Core area	The core area index is the percentage of core area in relation to patch area. A cell is defined as core area if the cell has no neighbour with a different value than itself (rook's case).	Configuration

Acronym	Level	Type	Description	Measures
Core area index (cai)	Class	Core area	Area within a patch that is not on the edge. Describes patch area and shape simultaneously. CORE values ≥ 0, increases without limit as the patch area increases and patch shape simplifies.	Composition
Standard deviation of patch core area (Core_sd)	Class	Core area	It equals the standard deviation of the core area of each patch belonging to class i. The core area is defined as all cells that have no neighbour with a different value than themselves (rook's case). The metric describes the differences among patches of the same class i in the landscape.	Configuration
Cpland	Class	Core area	It is the percentage of core area of class i in relation to the total landscape area. A cell is defined as core area if the cell has no neighbour with a different value than itself (rook's case). Because CPLAND is a relative measure, it is comparable among landscapes with different total areas.	Composition/ Complexity
Dcore_mn	Class	Core area	NCORE counts the disjunct core areas, whereby a core area is a 'patch within the patch' containing only core cells. Equals DCORE_MN = 0 if NCORE = 0 for all patches. Increases, without limit, as the number of disjunct core areas increases.	Configuration/ Complexity
Area_mn	Landscape	Area and edge	Individual patch area. Basic but important metric to characterise a landscape.	Composition
Aggregation index (ai)	Landscape	Aggregation	It equals the number of like adjacencies divided by the theoretical maximum possible number of like adjacencies for that class summed over each class for the entire landscape. The metric is based on the adjacency matrix and the single-count method	Composition/ Complexity
Core area index (cai)	Landscape	Core area	Area within a patch that is not on the edge. Describes patch area and shape simultaneously. CORE values	Composition

Acronym	Level	Type	Description	Measures
			≥ 0, increases without limit as the patch area increases and patch shape simplifies.	
Mean of related circumscribing Circle (circle_mn)	Landscape	Shape	Summarises the landscape as the mean of the related circumscribing circle of all patches in the landscape. CIRCLE describes the ratio between the patch area and the smallest circumscribing circle of the patch and characterises the compactness of the patch.	Compactness
Prd (patch richness density)	Landscape	Diversity	One of the simplest diversity and composition measures. It is a relative measure that is comparable among landscapes with different total areas.	Composition, Diversity
SHDI (Shannon's diversity index)	Landscape	Diversity	Widely used metric in biodiversity and ecology and takes both the number of classes and the abundance of each class into account	Diversity
SHEI (Shannon's evenness index)	Landscape	Diversity	Ratio between the actual Shannon's diversity index and and the theoretical maximum of the Shannon diversity index. It can be understood as a measure of dominance.	Dominance

7.3 Final Specification of EO solution

The developing field of landscape ecology has provided a strong conceptual and theoretical basis for understanding landscape structure, function, and change. Landscape ecology involves the study of landscape patterns, the interactions among patches within a landscape mosaic, and how these patterns and interactions change over time. With the use of landscape metrics, these principles from landscape ecology can be applied in a tangible, numerical way to formulate and solve real-world problems. Although there are known limitations to the use and applicability of landscape metrics (e.g. landscape and patch definition heavily context-dependent; results are scale dependant and difficult to transfer), they can offer a great potential for forest characterisation and monitoring, not to mention the integration of spatial pattern information in management processes.

The landscape metrics utilized in this analysis were calculated using established indices and commonly used software tools in landscape ecology. The data required for the analysis included spatial data sets representing land cover classes and appropriate boundary delineations (Table 10).

Table 10. Input datasets for Forest Landscape Metrics

Dataset	Use	Characteristics
Copernicus Global Land Service	Classification of land cover out of which the forest classes for	Coverage: Global

Dataset	Use	Characteristics
	the entire world can be extracted	Single layer, GeoTIFF files. CRS: EPSG 4326 Resolution: 100 m Version: 3.0 Product years: 2015-2019 Twelve forest classes
Global Administrative Areas (GADM)	Helpful in the standard delineation of landscapes across different regions	Coverage: Global Shapefile/Geopackage Version: 4.1 Up to four administrative levels

The forest classification provided by the Copernicus Global Land Service is the default classification layer for the calculation of landscape metrics. This layer, together with a user-defined area of interest (AOI), are the most important input parameters for the algorithm to run. The possibility of implementing of a user-defined forest classification instead of the default option is currently being tested.

The output obtained after running the tool is a combination of landscape metrics (in .csv and .shp formats, but also summarised in maps and plots). This allows researchers to gain a more comprehensive understanding of the landscape patterns, including patch abundance, size, configuration, interspersion, diversity, and edge habitat. It is important for the user to consider the strengths and weaknesses of each metric to gain a holistic understanding of its capabilities and limitations. To this end, accompanying information on the on each metric is also provided as an output after running the tool.

< END OF DOCUMENT >